aerospace

MDPI

Review

Electric Propulsion Methods for Small Satellites: A Review

Dillon O'Reilly [1], Georg Herdrich [2] and Darren F. Kavanagh [1,*]

[1] Faculty of Engineering, Institute of Technology Carlow, Kilkenny Rd, R93 V960 Carlow, Ireland; c00193552@itcarlow.ie
[2] Institut für Raumfahrtsysteme/Institute of Space Systems (IRS), University of Stuttgart, Pfaffenwaldring 31, 70569 Stuttgart, Germany; herdrich@irs.uni-stuttgart.de
* Correspondence: dfkavanagh@ieee.org; Tel.: +353-(0)59-917-5000

Abstract: Over 2500 active satellites are in orbit as of October 2020, with an increase of ~1000 smallsats in the past two years. Since 2012, over 1700 smallsats have been launched into orbit. It is projected that by 2025, there will be 1000 smallsats launched per year. Currently, these satellites do not have sufficient delta v capabilities for missions beyond Earth orbit. They are confined to their pre-selected orbit and in most cases, they cannot avoid collisions. Propulsion systems on smallsats provide orbital manoeuvring, station keeping, collision avoidance and safer de-orbit strategies. In return, this enables longer duration, higher functionality missions beyond Earth orbit. This article has reviewed electrostatic, electrothermal and electromagnetic propulsion methods based on state of the art research and the current knowledge base. Performance metrics by which these space propulsion systems can be evaluated are presented. The article outlines some of the existing limitations and shortcomings of current electric propulsion thruster systems and technologies. Moreover, the discussion contributes to the discourse by identifying potential research avenues to improve and advance electric propulsion systems for smallsats. The article has placed emphasis on space propulsion systems that are electric and enable interplanetary missions, while alternative approaches to propulsion have also received attention in the text, including light sails and nuclear electric propulsion amongst others.

Keywords: CubeSat; satellite; electric; propulsion; thruster; review; interplanetary; electrostatic; electromagnetic; electrothermal; light sail; nuclear

Citation: O'Reilly, D.; Herdrich, G.; Kavanagh, D.F. Electric Propulsion Methods for Small Satellites: A Review. *Aerospace* **2021**, *8*, 22. https://doi.org/10.3390/aerospace8010022

Received: 7 November 2020
Accepted: 12 January 2021
Published: 18 January 2021

1. Introduction

Enabling propulsion systems for satellites below 500 kg, considered small [1], is necessary for advancement into the solar system [2]. CubeSats, for example, are U class satellites defined by masses that typically weigh less than 1.33 kg per U. A 1 U CubeSat is 10 × 10 × 10 cm, a 2 U is 10 × 10 × 20 cm, 3 U is 10 × 20 × 30 cm and 12 U is 20 × 20 × 30 cm. These advancements are important for long term survival, identification of space resources and to develop new scientific objectives. Chemical propulsion systems used on the SpaceX's Falcon Heavy or NASA's Space Launch System (SLS) have low specific impulses (I_{sp}) thus poor fuel efficiency, very high thrust, short acceleration times and high mass [1,3]. Electric propulsion (EP) has higher fuel efficiency so less fuel and propellant storage is required, hence EP is more suitable for smallsats [4–6]. Propulsion provides smallsats with; collision avoidance [7,8], orbital manoeuvring, station keeping, orbit transfers, formation flights [9] and interplanetary trajectories as demonstrated by ESA's SMART-1 mission [10] and the Mars Cube One mission which was successfully completed this year [11]. Traditional smallsats orbit in low Earth orbit (LEO) and rely on reaction wheels and magnetorquers to provide attitude control and stability [12] for instruments. They cannot manoeuvre, transfer orbits or design safe de-orbit strategies nor can they go interplanetary. Interplanetary smallsat missions are becoming more popular with 13 cubesats planned to launch on the Artemis 1 mission in 2021 [13]. To provide effective propulsion for smallsats, the available on board power [14], the volume, size and weight, electromagnetic interference, cost-effectiveness [15] and the mission goals [16] should be considered. Interplanetary smallsats, require additional radiation tolerance and telecommunications design [13]. Advancements in very large scale integration (VLSI) electronics has allowed for the miniaturisation of smallsats [4]. Large constellations [17] performing remote sensing, weather predictions, pollution monitoring and improving communications in rural areas are being privatised. Large constellations can also expand our capability in observational and instrumental astronomy, allow for large planetary sensor arrays and provide huge interferometric bases [18]. Constellations comprising of thousands of smallsats, in general, will have much broader potential in comparison to single task satellites [9]. There is a growing demand for robust, cheap, high change of velocity and easily interfaced low power space propulsion systems to enable more competitive constellations. Challenges arise here in relation to erosion of outlet chambers, increasing thrust with minimal fuel and power, scaling to smaller volumes, creation of required material properties for in-space use [4,19], long distance communications [20] and others more specific to the chosen system. Moreover, large constellations can obstruct ground-based telescope observations. Space EP is defined as any system that accelerates a propellant through the conversion of electric potential energy into kinetic energy. Broadly, this energy conversion can be electrostatic, electrothermal, or electromagnetic based. It could also be a combination of both (e.g., electrothermal coupled with electromagnetic). This paper provides an overview of various space propulsion systems, under four major thematic areas as illustrated in Figure 1, with respect to smallsats and discusses avenues for improvement. Nuclear is included to explore alternative power sources for electric propulsion, while light sails are also included to highlight their smallsat applicability.

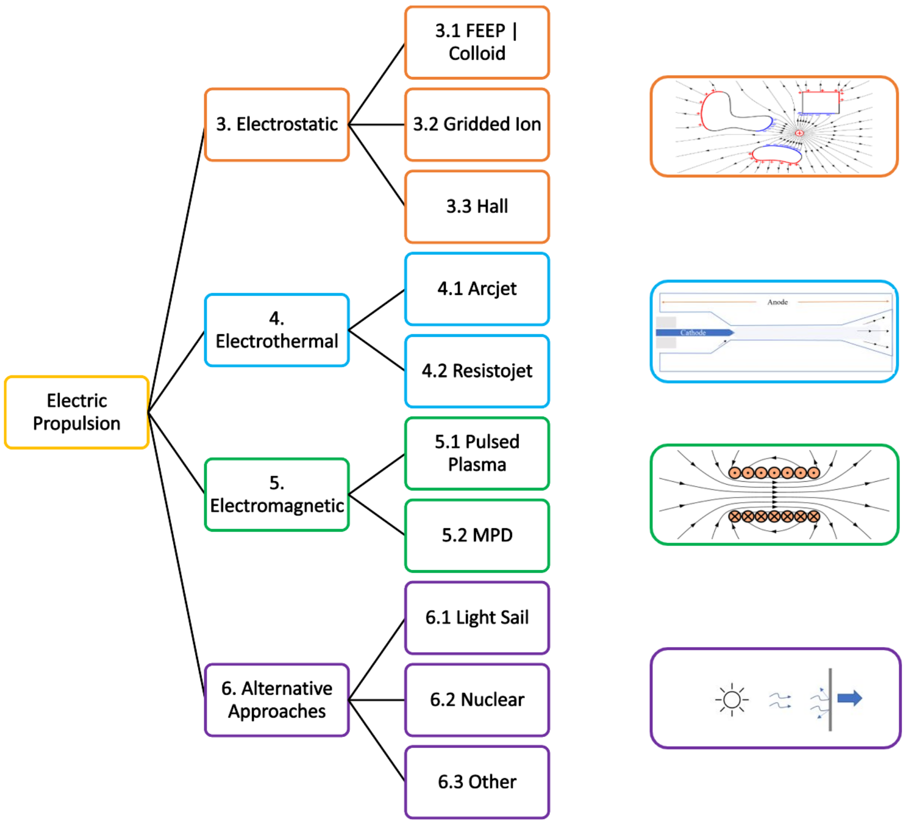

Figure 1. Describes the EP systems which this paper will review. Electric propulsion can be distinguished by the underlying physics which propels the system whether it be electrostatic, electrothermal or electromagnetic. Alternative approaches describes some additional propulsion systems that are currently under development.

2. Performance Characteristics

Spacecraft stay, manoeuvre or switch orbits using thrust. Thrust, is generated by the change of momentum of a substance, due to a chemical reaction or electrical principle. Thrust shows how much force, in newtons (N), that the propulsion system will move the spacecraft with. Assuming the propulsion system has a nozzle, thrust can be calculated using Equation (1) [1,14,16]:

$$Thrust,\ \tau = \dot{m} v_e + (P_e - P_a)\, A_e \tag{1}$$

Here, $\dot{m}$ is the speed at which the mass flows out of the nozzle, known as mass flow rate; P_e is the pressure at the exit of the nozzle while P_a is the ambient outside pressure, approximated at 0 for in-space conditions [16] and A_e is the area of the exit nozzle. The average velocity exiting the nozzle of the thruster, labelled v_e, is the product of specific impulse I_{sp} times the gravity due to earth g_0 at 9.81 m/s^2 and can be calculated by using Equation (2) below:

$$v_e = I_{sp}\, g_0 \tag{2}$$

The specific impulse I_{sp}, can be calculated using Equation (3):

$$I_{sp} = \frac{\tau}{\dot{m}\, g_0} \tag{3}$$

In general, the higher the specific impulse the less fuel that is required [21]. With this information, the change in velocity as a result of the force acting on the spacecraft due to the propulsion system can be calculated according to Tsiolkovsky [21] with Equation (4):

$$\Delta v = I_{sp}\, g_0 \ln \frac{m_i}{m_f} \tag{4}$$

Here Δv is the change of velocity of the spacecraft, m_i is the initial mass of the spacecraft and m_f is the final mass of the spacecraft. Equation (4) assumes continuous thruster operation and does not account for key differences between chemical and electrical propulsion [16]. To account for electric thrusters only. Considering electrostatic, electrothermal and electromagnetic variations: the thrust can be generally estimated using Equation (5) by selecting an arbitrary I_{sp}, for example in Tables 1, 2 or 3. η_t is the thrust efficiency and P_t is the power input [22]:

$$\tau = \frac{2\, \eta_t\, P_t}{I_{sp}\, g_0} \tag{5}$$

This equation can then be used to determine the propellant mass flow rate of electric thrusters:

$$\dot{m} = \frac{\tau}{I_{sp}\, g_0} \tag{6}$$

The lower end of the maximum mission duration t_{burn} and the delta v for an EP system can then be estimated by assuming a propellant mass, m_p and spacecraft dry mass m_d:

$$t_{burn} = \frac{m_p}{\dot{m}_p} \tag{7}$$

$$\Delta v = I_{sp}\, g_0 \ln\left(\frac{m_d + m_p}{m_d}\right) \tag{8}$$

Range and Application

A highly accurate method to determine the performance of a thruster for a specified mission at a systems level approach for smallsats exists [23]. Mass, power availability, trajectory options, thrust duration, thermal requirements and various other trade-off parameters critical to a missions lifetime are compared. It is a baseline modelling framework for investigating U class CubeSats for Earth escape trajectories. As a first-order mission design estimation to assess range and capability, assuming a constant thrust as is usually the case with long EP missions, Equation (9) can be used:

$$t_{tr} = \frac{\Delta m \; v_e}{\tau} \tag{9}$$

Here, t_{tr} is the mission duration and Δm is the change of mass over the mission duration due to propellant loss, Δm can be approximated using Equation (10) [22]

$$\Delta m = \int_0^{t_{tr}} \left(\frac{t}{v} \right) dt \tag{10}$$

3. Electrostatic

In the case of electrostatic thrusters, electrical power is first used to ionise the propellant for plasma production. The ions are then accelerated using electrodes that apply an electric field to the ions for plasma acceleration [24].

3.1. Electrospray Thrusters

An ionic liquid of charged particles is sprayed onto a sharp tip in one of three possible ways: externally wetted, porously or through a capillary. Ions or droplets are then drawn from the tip using a metal extraction plate. The ions form a cone shape, known as a Taylor cone, as they are drawn from the tip. The ions are then passed through a static electric field to accelerate them. The field is created by the potential difference between an emitter and extractor grid with a max potential difference determined by the Child Langmuir law [1]. Multiple Taylor cones in an array make up the thruster, the potential to have many Taylor cones makes these thrusters adaptable [25]. Electrospray thrusters operate in either droplet or ion emission mode. They generally come in three different variations which are characterised by the propellant being used. This largely determines if a neutralizer is needed to keep the spacecraft charge neutral. The neutralizer emits electrons into the exhaust to neutralise the particles. Colloid based thrusters, as shown in (b) of Figure 2 and in Figure 3, typically emit larger charged droplets (droplet mode) using a propellant that is charge neutral. Some colloid thrusters may also require a neutralizer if the propellant is not doped with a salt which increases electrical conductivity. Field Emission Electric Propulsion (FEEP) thrusters, as shown in (a) of Figure 2, typically emit individual ions (ion emission mode) and require a neutralizer as they operate with a liquid metal demonstrated in Figure 4. FFEP thrusters offer high thrust precision but low thrust forces (<1 mN) and a wide range of specific impulses [26]. The final type of electrospray thruster is Ionic Liquid Ion Source (ILIS) which does not need a neutraliser as it only uses molten salts as propellant. To calculate the thrust and exit velocity of an electrospray thruster, see Equations (11) and (12) [14].

$$v_{e_i} = \sqrt{2 \; \mathrm{V}_i \; I_i \; \frac{m_{\text{ion}}}{q}} \tag{11}$$

$$\tau = \dot{m}_{\text{ion}} \; v_{e_i} = \sqrt{2 \; \mathrm{V}_i \; I_i \; \dot{m}_{\text{ion}}} \tag{12}$$

Here, $\frac{m_{\text{ion}}}{q}$, is the mass-charge-ratio; I_i is the ion beam current and V_i is the ion accelerating voltage. Some examples of electrostatic thruster parameters are presented in Table 1.

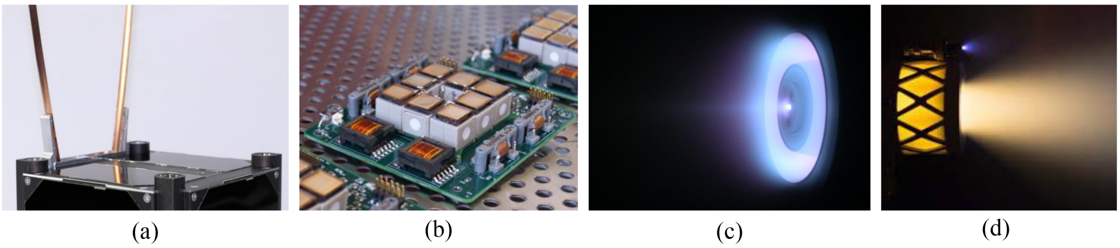

Figure 2. Electrostatic thruster examples: (**a**) NanoFEEP thrusters integrated into the rails of the flight model of the UWE-4 CubeSat, size 3 cm^3 [7], (**b**) S-iEPS propulsion module electrospray microthruster, size [14.4 × 14.4 × 14.1] mm [27,28], (**c**) Halo is a miniaturised center line-cathode Hall thruster, size 7.5 cm in diameter credit: ExoTerra Resource LLC and (**d**) BIT-3, the world's first iodine-fueled gridded ion thruster, size 2.5 cm in diameter [29].

Table 1. Examples of electrostatic thruster parameters.

Name	Type	Specific Impulse (s)	Thrust (N)	Power (W)	Propellant	Mission Demo	Manufacturer
			Electrostatic Thrusters				
ST7	Colloid	>150	5–36 µ	∼2	Ionic liquid	LISA Pathfinder	Busek [30]
pet-100-mk2	Colloid	>7500	220 µ	∼14	EMIM	Experimental	UoSH [31]
S-iEPS/ TILE	ILIS	1150	0.1 m	<0.15	EMI-BF4	AeroCube 8	MIT/Accion [27]
nanoFEEP	FEEP	6000	8 µ	50–150 m	Ga	UWE-4	Dresden [7]
AIS ILIS1	ILIS	4500	3 µ	<0.1	Molten Salts	Experimental	Applied Ion [32] Systems
PPS-1350 G	Hall thruster	1660	90 m	1500	Xe, Kr, Ar	SMART - 1	Safran [33]
PPSRX00	Hall thruster	1450	40 m	650	-	Experimental	Safran [34]
SPT-50M	Hall thruster	1200	18 m	300	Xe	Canopus-V	Fakel [35]
HT100	Hall thruster	1300	9 m	175	Xe	Experimental	SITAEL [36]
BHT-200	Hall thruster	1390	13 m	200	Xe, Ar	Falconsat-5	Busek [29]
NSTAR Ion	GIT	3100	92 m	2.3 k	Xe	Deep Space 1	NASA [37]
BIT-3	RF GIT	1400	0.66 m	56	I	SLS EM-1	Busek [38]
MiXi	GIT	3000	1.43 m	30	Xe	Experimental	UCLA [22,39]

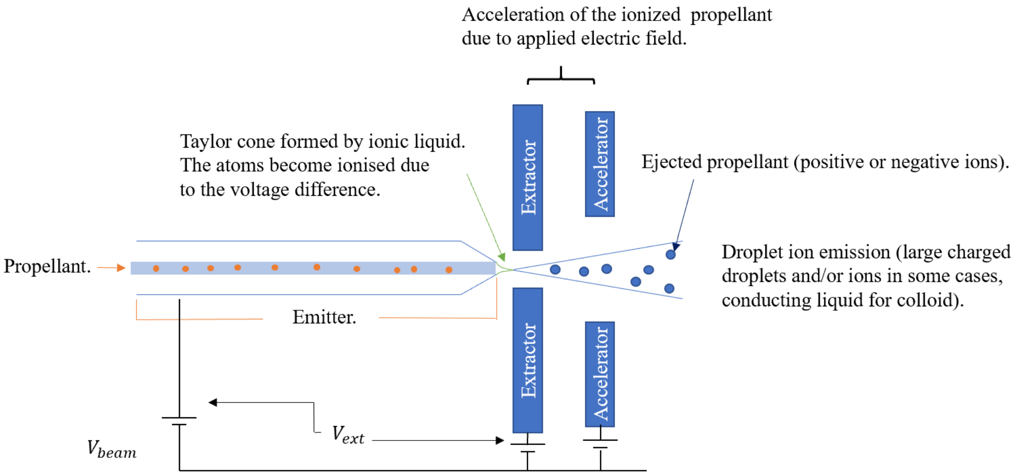

Figure 3. A molten salt (colloid or ILIS) based thruster as a simplified schematic diagram.

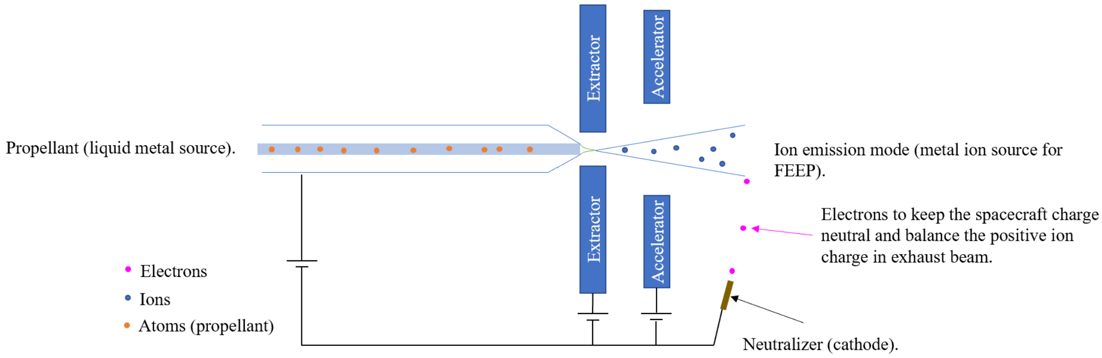

Figure 4. A FEEP thruster as a simplified schematic diagram. Addition of a neutralizer and metal ion source in comparison to Colloid electrospray thruster.

Most recent works on electrospray thrusters have focused on increasing lifetime, thrust and investigations of various array configurations. Electrospray thrusters suffer shortened operating lifetimes due to impingement of ionised propellant onto the extractor and accelerator grids. The high voltages required, results in electrochemical degradation [40,41]. Lifetime can be improved by alternating the emission polarity of the thruster head [42], lowering the propellant flow rate [43] and reducing the conductivity. Exploring better emitter designs for improved performance can be simulated using the models referenced in [44]. Electrospray propulsion dampens perturbations and noise on board the spacecraft which is one of the primary reasons these thrusters were chosen for the LISA pathfinder mission. During this mission issues arose. One thruster experienced high current transient disturbances due to noise. This could be resolved by increasing the dynamic range (dB) of the Analogue to Digital Converter (ADC) used within the control system. However, this remains to be experimentally validated. Thrust could be increased by increasing the number of Taylor cones [45]. Decreasing the size of the Taylor cones is advantageous as it decreases mass and allows for more redundant systems (fail-safes) to increase the reliability [1]. NanoFEEP demonstrated the first electric thruster on board a 1 U CubeSat with power margins applicable to a picosat within the 50–150 mW power range. It produced continuous thrusts of 8 µN and weighed a total of 6 g. This is achieved partly by using gallium as the propellant [46]. However, issues arose with the propellant heaters not producing adequate active thrust duration to enable continued operation. One particular research avenue to consider is how to optimally arrange the Taylor cones into arrays and which configurations and manufacturing methods offer the best performances [47].

3.2. Gridded Ion Thruster

Gridded ion thrusters (GIT) date back to the 1960s. They were first proposed by Tsiolkovsky in 1911. A GIT produces ions by bombarding a propellant with a high energy electron beam created either by a direct current (DC) discharge, a radio frequency (RF) discharge or a microwave (MW) discharge [48]. The ions are then ejected through a series of electrically charged grids. A potential difference is established between these grids, one a screening grid and another an accelerating grid as shown in Figure 5. This potential difference is what determines the acceleration of the propellant. The negatively charged anions created are accelerated by the cathode grid (accelerator). The most common type of propellant is xenon (Xe) though earlier versions of this thruster used metallic propellants such as mercury or cesium which have high atomic masses, ionize easily but have very high boiling points and are toxic chemicals. Xenon, in comparison to cesium and mercury, ionises more easily, has a high atomic mass and critically, and it has a low boiling point [49] making it more favourable. Ion thrusters have the highest efficiency in comparison to other propulsion methods and very high specific impulses. The thrust and exit velocities can be calculated using Equations (13) and (14).

$$v_{e_i} = \sqrt{\frac{2q\mathrm{V}_i}{m_{ion}}} \tag{13}$$

$$\tau = \sqrt{\frac{2m_{ion}\mathrm{V}_i}{q}} I_i \tag{14}$$

The exit velocity is a function of the propellant charge q, the mass of the propellants ions m_{ion} and the ion accelerating volatge V_i. I_i is the ion beam current for estimations of thrust.

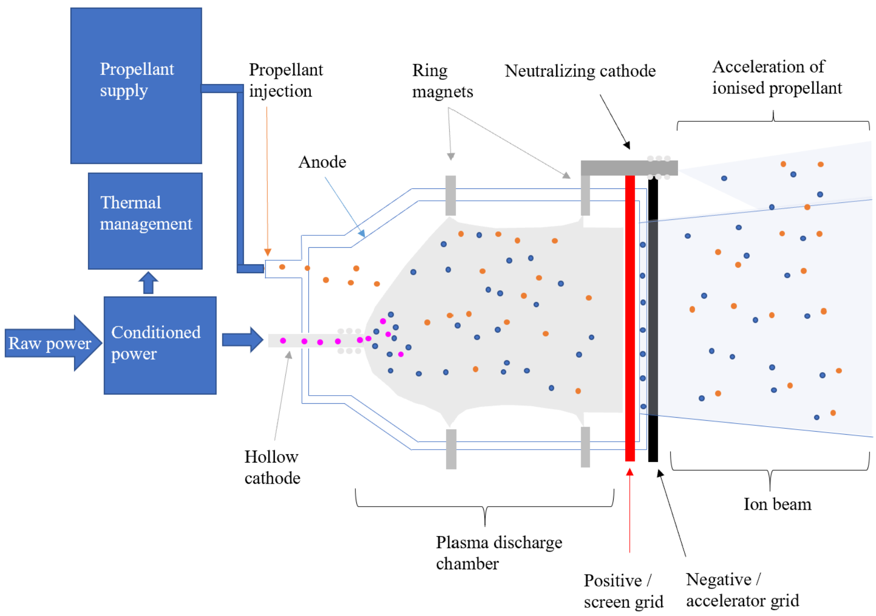

Figure 5. A two grid Gridded Ion Thruster (GIT) as a simplified schematic diagram.

Within the past two years, research for GITs has focused on development of subsystems such as the PPU, improvement of plasma modelling parameters within simulation environments and identification of alternative propellants. These focus areas have allowed for broader functionality across operating modes, more realistic models and propellants with higher I_{sp} than xenon under specific conditions. With regard to the power processing unit (PPU) which is used to provide power to the electron beam required to ionise the propellant [50]. A newly developed commercial PPU being used on NASA's first planetary defence mission, the Double Asteroid Redirection Test (DART), allows smallsats to escape the Earth's orbit because it operates over a wider range of 60–160 V with 7 kW of power in comparison to more traditional PPUs [51]. By offering a wider voltage output range the thruster can operate between orbit raising and station keeping operational modes. The PPU performance is dependent upon the power density, voltage output range and current form factor [50]. The broader voltage output range is achieved by using a Dual Active Bridge (DAB) circuit topology [51]. Future GITs with broader PPU operating ranges will be needed to enable higher orbit raising and Earth escape. Modelling of the plasma currents, density and voltage potential is important to identify problem areas, these parameters are difficult to obtain experimentally. Thus, numerical simulation methods are used [52]. Improvements to these models by increasing the permittivity, reducing the mass of heavy particles and scaling down the thruster system are needed [52]. With these improvements, comparing and contrasting various parameters within the models will become faster, more reliable and allow for the selection of more impactful experimental work. Another recent and interesting development is the staging of GITs to enable interplanetary missions for smallsats [53]. Staging increases the delta velocities by reducing mass as each stage is completed [54]. This allows smallsats to escape Earths orbit from a geostationary orbit (GEO). Staging of electric thrusters can be performed with staged ion thruster layers that are jettisoned off as the propellant is depleted. Reducing the size and weight of the system is therefore highly desirable. The size and weight can be further reduced by the application of a radio frequency (RF) voltage signals on the grid. This allows for a continuous ion beam which removes the need for a neutraliser thus reducing the size and weight further [55]. As mentioned earlier, xenon is the typical propellant used but using iodine as a propellant under a low flow regime creates more thrust than xenon at similar operating powers [49,56]. The iodine radiofrequency ion thruster (IRIT4) from reference [56], produced 2.3 mN of thrust, a 2361 s specific impulse with nominal power of 95.8 W and grid voltages of 1800 V. Although iodine is a corrosive propellant [49], it is more abundant and cheaper than xenon which currently costs around USD 850/kg. As more satellites go into orbit, this cost is only set to increase. The first iodine fuelled GIT is shown in Figure 2, (d) above. Water was also explored as a propellant for GITs. While the performances did not compare to that of xenon or iodine, water is a safer propellant and an abundant fuel source [57]. There is a fast and cheap screening method for assessing new propellants that exists in reference [49], though any new propellant needs to also be experimentally validated including the adaptions to grid geometries and whole diameter distributions. Investigating the properties and applicability of new propellants will become quite important as the growth of smallsat increases. The referenced model requires a thorough understanding of the microscopic processes inside the plasma to really validate any potential molecular propellant. Molecular propellants offer a much broader potential list of alternatives. However the drawback of these propellants is that they require a lot of plasma and beam diagnostics due to the large amount of microscopic processes [49]. In the future, it will be more important to have alternative propellant options available.

3.3. Hall Thruster

Hall thrusters (HT), alternatively called stationary plasma thrusters (SPT), are based on the Hall effect principle [58]. This thruster accelerates the propellant to a high velocity as it passes through an electric field in a channel generated perpendicular to the magnetic field. The channel is shown in orange of Figure 6. The magnetic field limits electrons from spinning on their own axis (axial motion) to avoid shorting of the electric field, it also confines them. The electrons, stored in a channel at the exit of the thruster, are used to ionise the propellant which is fed through the anode. The plasma at the open end of the exhaust provides the negative charge which accelerates the ions instead of a grid as in GITs. The efficiency is typically less than that of GIT, however the thrust is often higher for a given power and the required power supplies are less demanding [59]. Hall thrusters can be broken down into either a stationary plasma thruster (SPT) or a thruster with anode layer (TAL) [60]. The SPT HT has an extended acceleration zone while TAL HT has a more narrow acceleration zone. With regards to power generation, not only for HT but for most EP systems, they are typically powered by solar cells which attach to a keeper (the power regulator) which is responsible for ignition of the thruster. Hall thruster exit velocity and thrust can be calculated using Equations (13) and (14).

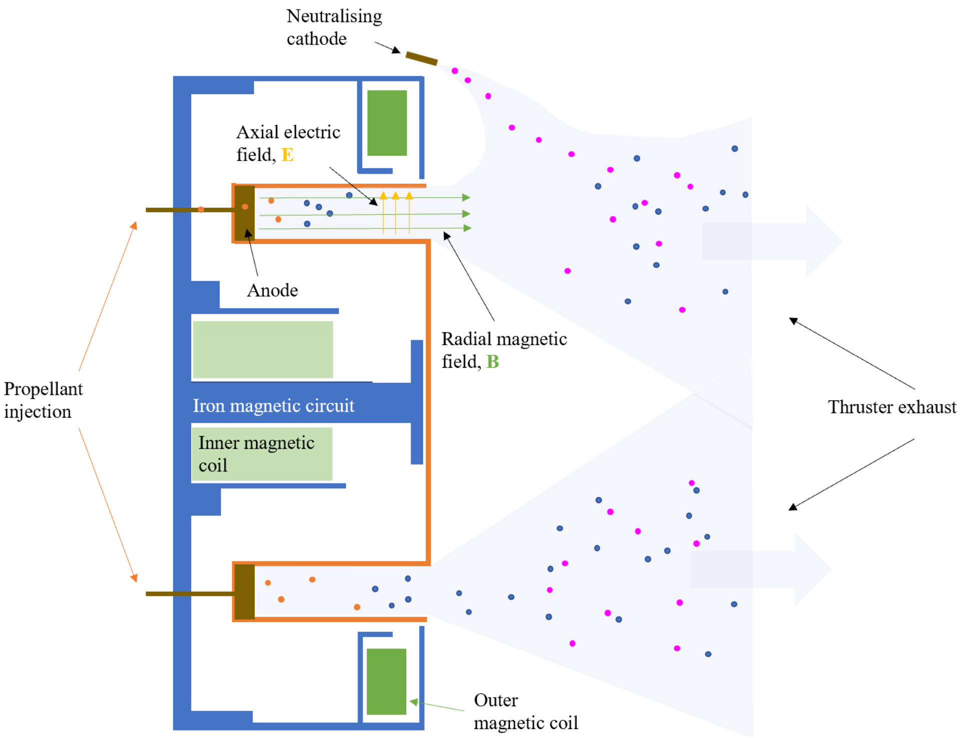

Figure 6. A simplified schematic diagram of a TAL HT or if the channel is extended this would become a SPT HT.

Hall thrusters operate in different modes, each mode has different characteristics and in recent years these modes along with lifespan parameters have been extensively investigated. It should be noted that the hall thruster is already a proven method of enabling smallsat based interplanetary missions. For example, the ESA SMART-1 mission (Small Mission for Advanced Research in Technology) used a Hall thruster to escape Earth orbit and reach the moon with a small satellite that weighed 367 kg [33]. As satellites get smaller and lighter however, it remains questionable if they can be significantly effective below 367 kg. Similar to GITs, analysis of the plasma is helpful to improving performance. An experimental analysis of the plasma in HTs using cameras [61] shows that the transitions, caused by changes in the cathode emissivity, between operating modes; nominal, higher than transition and lower than transition; is when plasma fluctuations most frequently occur. Each transition produces various discharge currents, extraction voltages (potential difference between anode and plume) and associated changes to the emissivity properties of the cathode. Currently, it is not understood why the extraction voltage changes in various transition modes, why current oscillations disappear in lower than transition mode (breathing mode) and why there are plasma gradients during various transition modes [61]. Classifying and characterising the relationships between the parameters responsible for transition mode performance would be a significant contribution to the field. Since each transition mode has a different effect on thruster erosion, lifespan limiters are poorly understood in HTs [62]. One method of combining these experimental findings with numerical estimations [62] to improve thruster performances, lifespan and operating conditions is by coupling data-driven models with machine learning (ML) algorithms. Predictive modelling of thruster erosion has yet to be achieved in this capacity [63]. The need for analytical models to study HT operation and provide predictive analytical frameworks continues to increase [64]. HT can be modelled under fluid or kinetic regimes and while 2D modelling of HTs has been achieved, 3D modelling using particle-in-cell monte carlo collisions (PIC MCC) remains difficult and heavily time consuming, often taking up to several months to complete [65]. One method to reduce simulation time may be to take advantage of recent advances in quantum computing for monte-carlo simulations applied to HT. The complexity of electrons colliding with the inner walls of the thruster has prevented the development of predictive modelling softwares [65] but with improvements to computing power and taking into consideration the various parameters detailed in reference [65], more realistic models could be achieved. Varying the strong magnetic field around the cathode, which is used for ignition and discharge of the plasma, could also help to reduce erosion and improve lifetime [66]. Hollow cathodes, as shown in (c) of Figure 2, however, typically have a long life and offer robust performance [59,67]. For small satellites with low power, a heaterless hollow cathode is a popular choice as it reduces weight, has a compact size and is suitable under low power conditions [68]. Various configurations of the magnetic and electric fields provide shielding to prevent erosion in the discharge chamber which is caused due to ion flux and ion energy at the wall [63]. Many configurations have been explored with some less mature HTs such as: the wall-less hall thruster [69] and the cusped field plasma thruster [70]. The choice of materials used at the walls is also a potential avenue to improve the lifetime and performance, in particular selecting materials with low sputtering yield [63]. Nano-materials could be engineered to provide low sputter yield or self-healing properties at the wall [4], this offers an exciting prospect which has yet to be developed and realised. The nano-materials could also be used in many other parts of the propulsion system. While the propellants are typically xenon or krypton for HTs [71], with some systems employing both [72] selecting propellants which are more abundant and cheaper will also be important for HT.

4. Electrothermal

In electrothermal systems, electrical power is first used to heat propellant in a chamber. The propellant is then expanded through a converging/diverging nozzle for acceleration [24].

4.1. Arcjet

A constant current is passed through two electrodes of opposite polarity at either end of a constricting tube to induce a sustained electric arc, this heats the propellant to exit through a diverging nozzle at high velocity [73]. Typically, the first part of the nozzle and the nozzle constrictor is the anode, mounted to a co-axial tube at the end of which is a cathode rod, the electrodes are separated by a high temperature insulator such as boron nitride or aluminium oxide [73]. The arc is ignited by a high voltage, usually 1000–4000 V and then dips to either a low operating mode, 30–50 V or a high voltage operating mode, 80–160 V. Arcjets typically have four power levels ranging from very low, 100–300 W to high power, 30–200 kW. The most suitable power range for smallsats is at the lower end of the power scale, within the 100 W–1 kW range arcjets, as shown in the top right of (a) in Figure 7 [74]. Since the arc can generate significantly higher temperatures in comparison to a heating coil, the specific impulse is usually greater than that of a resistojet and while similar to chemical thrusters, the arcjets also usually have 2–3 times higher specific impulses than chemical rockets [75]. On the other hand, arcjets have low efficiency and a lot of heat loss, they also typically require complex power processing PPUs, e.g Aerojet. The thrust of the arcjet, according to [76], can be estimated using Equation (1) and exit velocity using Equation (2) described in the performance characteristics section, though they do not account for frozen flow conditions. Some examples of electrothermal thruster parameters are presented in Table 2 while a simplified schematic diagram is shown in Figure 8.

Table 2. Examples of electrothermal thruster parameters.

Name	Type	Specific Impulse (s)	Thrust (N)	Power (W)	Propellant	Mission Demo	Manufacturer
			Electrothermal Thrusters				
MR-512	Arcjet	502	254 m	1.8 kW	N_2H_4	Flight Proven	Aerojet [77]
MR-502	Resistojet	304	0.5	840	N_2H_4	Flight proven	Aerojet [77]
ATOS	Arcjet	400	0.1	750	NH_3	Flight Proven	IRS, Stuttgart [78]
VELARC	Arcjet	865	22.5	365	H_2	Experimental	IRS, Stuttgart [79]
FMMR	Resistojet	65	1.2	<6	H_2O	Experimental	Uni. of S. California [80]
AQUARIUS	Resistojet	70	4 m	<20	H_2O	SLS EM-1 (2021)	Uni. of Tokyo [81]
STAR	Resistojet	79.42	29.8	28.55	Ar	Experimental	Uni. of Southampton [82]
Sagami 3	Arcjet	480	<50 m	300	NH_3	Flight Proven	ISAS [83]

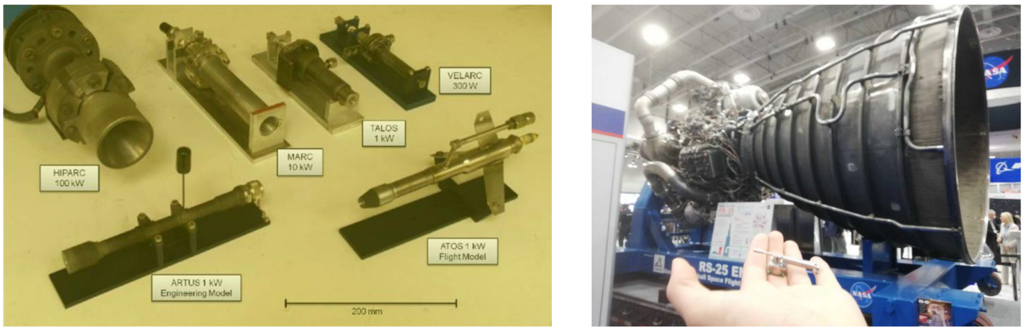

(a) (b)

Figure 7. Electrothermal thruster examples: (**a**) Arcjet thruster range at IRS (upper line from left: HIPARC 100 kW, MARC 10 kW, TALOS 1 kW, VELARC 300 W; lower line from left: ARTUS IM 3 engineering model, ATOS flight model), a scale bar is provided for size [83], (**b**) Single Orbital Thruster is the world smallest commercially available full in-orbit micro-resistojet thruster system, size 6 mm in diameter credit: Aurora Propulsion Technologies.

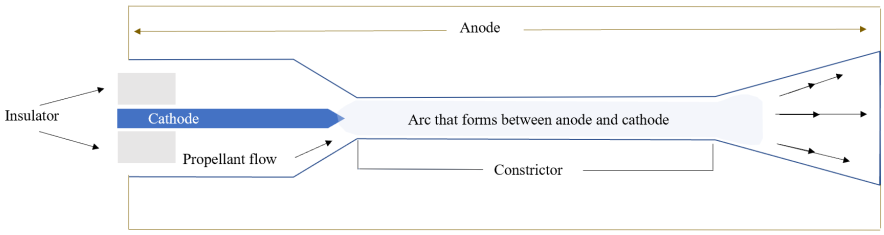

Figure 8. An arcjet thruster as a simplified schematic diagram.

Recent works for arcjets have focused on the usage of different propellants, reducing erosion to improve lifetime and alternative designs to enable higher thrust forces. The main life limiting factor for arcjets is ablation of the electrodes and the nozzle throat, in particular occurring at start up. The constrictor leads to a drift due to the increasingly reducing aperture. To be specific, it is the duration of the transfer process for the initial arc on the anode at start up, that is a key parameter for predicting how much 'life' the thruster has left. Recently, experimental work has found that increasing the propellant flow and decreasing the throat diameter, decreases this arc root transfer process, which improves longevity [84]. In comparison to electrospray thrusters, where lowering the propellant flow rate was shown to improve lifetime, as mentioned in Section 3.1. Another disadvantage of lowering the propellant flow for arcjets is that it reduces the specific impulse due to friction losses on the inner nozzle core [74]. Therefore, it should be noted that propellant flow rate is highly dependent on the chosen system. Arcjets are generally used for station keeping, although alternative designs have been proposed to increase the thrust forces. While most spacecraft operations are autonomous, when arcjets encounter abnormal operating conditions they require a spacecraft controllers input to analyse, decide and perform corrective maneuvers. Autonomy would reduce costs and remove the need for spacecraft controllers when encountering these abnormal operating conditions [74]. Autonomy could also produce more efficient usage of propellant in comparison to a controller under abnormal conditions. Using algorithms to autonomously predict optimal fuel sources for different thrusters could prove more robust. With regards to propellant, which is traditionally either hydrazine or hydrogen, a recent study found argon as an efficient low cost alternative [85]. Although the currents required were considerably higher than low power arcjets. It would be interesting to take this as a case study for a computer simulation model, basing any results on the experimental parameters. Hydrogen, though it has a higher cost, shows higher specific impulses in comparison to hydrazine or other fuel sources. Using a model to identify why and apply this model to other compounds might produce worthwhile new findings. Using hydrogen at low powers such as 365 W, has enabled 865 s specific impulse [74]. There is a significant potential to save mass and to increase efficiency of thermal arcjets making use of advanced additive manufacturing technologies. In reference [86] a nozzle design is reported that is based on Additive Layer Manufacturing (ALM) tungsten allowing for complex cooling channel technologies. These cooling channels can be used for regenerative cooling, i.e., where the propellant is fed through the channels in order to cool the nozzle and then the heated propellant is fed into the discharge chamber enabling an increase of the thermal efficiency of the thermal arcjet. This technology, however, necessitates light propellants such as hydrogen or helium due to the adequately high specific heat. Arcjets could play a very important role in both station keeping and de-orbiting of satellites. They are highlighted in the ESA CleanSpace initiative [78]. One possible reason for this is because arcjets are particularly suited to multi-mode propulsion systems in which more than one propellant is shared amongst the propellant feed system [87]. Enabling the arcjet to potentially utilise in-situ space resources or waste products from chemical rockets even when depleted of propellant. Identifying methods to lower the specific heat for some arcjets could therefore be advantageous in light of the ESA CleanSpace initiative.

4.2. Resistojet

A resistojet, shown in Figure 9 is very similar to cold gas thrusters (CGT) in that it simply releases a propellant under pressure. This propellant is first heated to a high temperature electrothermally, typically powered from solar panels which is directed towards a heating coil in the propellant tank [73]. The technology is simpler than an arcjet thruster [1]. The pressurised, high temperature propellant is released into space through a converging-diverging nozzle which accelerates the propellant to impart momentum on the spacecraft. Resistojets can be extremely small as shown in (b) of Figure 7. The thrust and specific impulse of the resistojet can be calculated using Equations (15) and (16).

$$\tau = A_0(\frac{n_0 K T_o}{2})x \tag{15}$$

$$I_{sp} = \sqrt{\frac{\pi k T_o}{2m}}\frac{1}{g_0} \tag{16}$$

This is the thrust at stagnation pressure [14], where the local velocity is zero as it passes through the throat, it depends on the stagnation number density of the propellant n_0, the stagnation temperature T_0, and the probability of a molecule (x) exciting the expansion area A_0. With Boltzmann constant k and g_0, the acceleration is due to gravity.

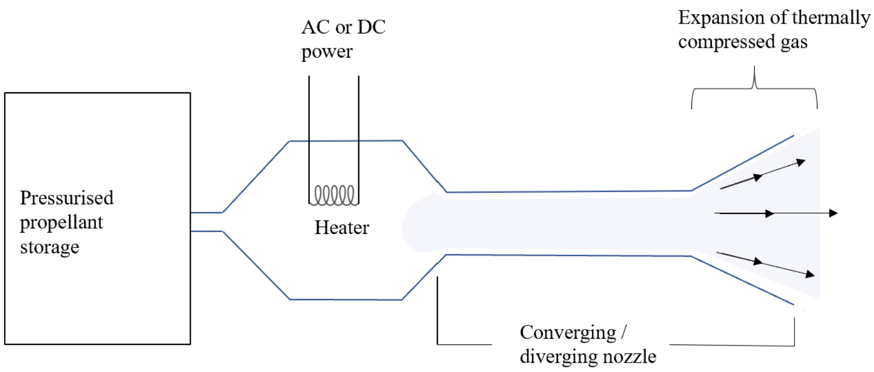

Figure 9. A resistojet thruster as a simplified schematic diagram.

Resistojets have been flight-proven since the 1960s. In recent years, research groups have focused on investigating different propellants, various materials for the ohmic heaters and trying to reduce the power requirements in order to scale into smaller satellites. More institutions are now opting for safer propellants such as water due to a growing demand in the aerospace industry for green-propellants. Green propellants are less likely to react under high temperature and pressure conditions experienced during launch [88]. A new water based resistojet called AQUARIUS from the University of Tokyo and JAXA managed 4 mN of thrust at 70 s specific impulse with just 20 W of power in ground testing [81]. Water will also be widely available as human expansion into the solar system continues, leveraging on the planned NASA artemis missions [89]. Water can be used as a propellant for other types of EP such as the GIT [90]. Hence, this could potentially enable dual mode propulsion systems between a resistojets and ion thrusters. Sloshing within the tanks of water propelled resistojets is a disadvantage to the stability and control of the satellite. Reducing the sloshing effect could reduce the amount of reaction control thrusters (RCS) required. Sloshing could be reduced by using a MEMS based low pressure micro-resistojet (LPM) system [80] or by optimising the baffle installation height and width [91]. Reducing the amount of propellant required for a particular mission is also advantageous and this could be achieved by reducing the stagnation temperature of the fuel [82]. The specific impulse of resistojets is limited by the melting temperature of the propellant used and by the maximum permissible temperature of the ohmic heater [75]. The choice of material for the ohmic heater or heat exchanger is therefore an important parameter [1]. Metal additive manufacturing processes has enabled a new area of research for these types of thrusters by enabling higher temperature heat ex-change capability, some even reaching 3000 K. Additive manufacturing improves the thrust and specific impulses achievable by integrating the heat exchanger with the nozzle as one single piece [92]. The super high temperature additive resistojet (STAR) thruster developed at the University of Southampton reached a specific impulse of 80 s, thruster efficiency >60% and thrust of 29.8 mN with argon as the propellant in initial tests. A spin-off from additive manufacturing is Monofilament Vaporisation propulsion used for resistojets [93]. This system is suited to smallsats with power ratings of 45 W and can generate 66 s specific impulse and 4.5 mN of thrust. It works by feeding the propellant to a vaporisation chamber in the same way a 3D printer feeds polymer into the heating discharge nozzle. The advantage of using a polymer, such as polyoxymethylene, is that it avoids freezing, over pressurisation and degradation [93].

5. Electromagnetic

Unlike electrostatic systems, electromagnetic systems ionise and accelerate the propellant under the combined action of magnetic and electric fields [24]. For this reason, these systems can often require higher power levels.

5.1. Pulsed Plasma Thrusters

A pulsed plasma thruster (PPT) as shown in (b) of Figure 10, works by accelerating an ionised gas through a magnetic field. The magnetic field is induced by a cathode and anode at the exhaust nozzle where an electric current flows to ignite the gas into a plasma and ejecting it, which imparts momentum on the spacecraft. PPTs have high specific impulses, low power consumption and low overall thrust. There are generally two types, thermal PPT's and hybrid/magneto-hydro-dynamic based PPTs. The PPT consists of three major components: the power supply, the power processing unit (PPU) and the energy storage unit (ESU) [94] shown in Figure 11. The power processing unit converts energy from the power supply, which usually incorporates solar cells, to charge the energy storage unit. Then a capacitor discharges the stored ESU energy when it is at maximum capacity, it then re-charges and repeats the cycle. Meaning the thruster itself only pulses periodically (10–20 μs) ablating, usually, a solid propellant [95]. Pulsed plasma thrusters have been demonstrated successfully on a number of in space missions particularly stemming from Russian research institutes for the past 50 years [96]. They date back to the 1960s and can be categorised into two design methodologies: (a) parallel plate for high energy (E > 20 J) (b) coaxial type for low energy designs (E < 20 J) [97]. The thrust for a pulsed plasma thruster may be calculated using Equation (17) [14]:

$$\tau = q\,(\tilde{\mathbf{E}} + \tilde{u}_i \times \tilde{\mathbf{B}}) + \sum (P_i)_k \tag{17}$$

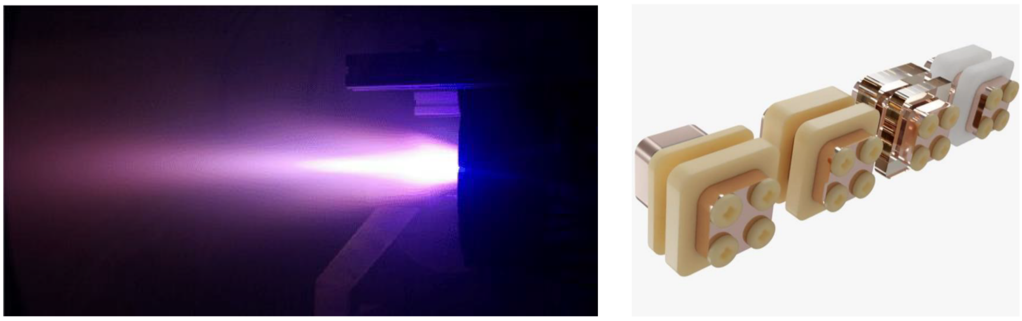

(a) (b)

Figure 10. Electromagnetic thruster examples: (**a**) IRS AF-MPD thruster ZT1 in operation, size 40 mm in diameter [79] (**b**) AIS-gPPT3-1C Single-Channel Gridded Pulsed Plasma Thruster, size [40 × 38 × 24] mm credit: Applied Ion Systems.

As mentioned above, the magnetic field produces a force on the charged particles which results in thrust, this force can be described by the Lorentz force in which a particle of charge, q, moving with a velocity, $\tilde{u}_i$, in an electric field $\tilde{\mathbf{E}}$ and a magnetic field $\tilde{\mathbf{B}}$, plus the sum of all collision forces per particle over all particles, $((P_i)_k)$ experiences a force which is equal to the thrust, τ. For the exit velocity, the radius of the anode, R_a and the radius of the cathode, R_c can be used, where η is the efficiency of the propellant and μ_0 is the permeability of free space. The I_{sp} can then be calculated using Equation (3) [14]. Some examples of electromagnetic thruster parameters are presented in Table 3.

Table 3. Examples of electromagnetic thruster parameters.

Name	Type	Specific Impulse (s)	Thrust (N)	Power (W)	Propellant	Mission Demo	Manufacturer
			Electromagnetic Thrusters				
APPT-250	APPT	1900	1.2 m	60–120	Teflon	Experimental	RIAME MAI [96]
ADD-SIMPLEX	iMPD	2761	1.373	<100	PTFE	Validated	IRS, Stuttgart [98]
PETRUS	iMPD	1567	41.46 μ	5–8	PTFE	Green Cube	IRS, Stuttgart [98]
BmP 220	PPT	536	0.14 m	<3	PTFE	FalconSat-3	Busek [14]
MPACS	PPT	827	0.144 m	<10	PTFE	Falconsat-3	Busek [14]

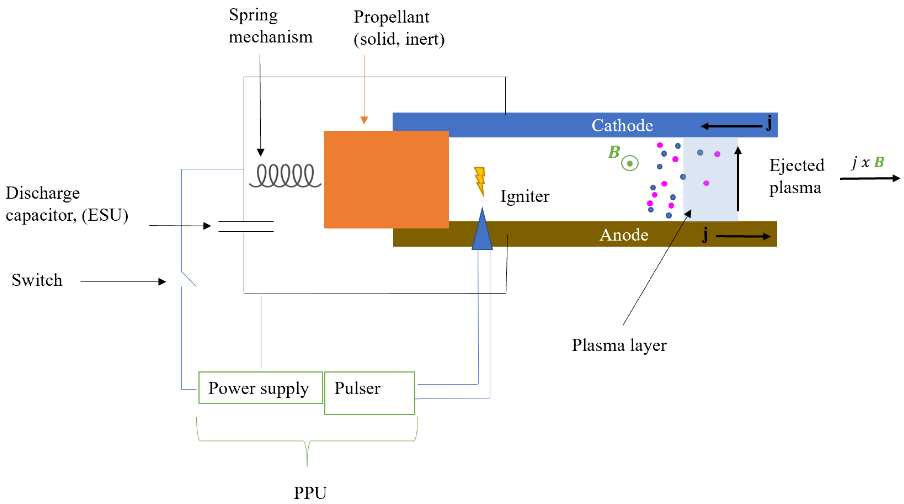

Figure 11. A parallel plate pulsed plasma thruster as a simplified schematic diagram.

Pulsed plasma thrusters have a long heritage dating back to 1964 with Zond 2 and then subsequently Zond 3. PPTs are optimal for station keeping and drag makeup for smallsats [99] and there remains many research avenues in which to improve the overall efficiency and cost of PPTs [100]. Recent work on propellants has shown promise for improving the I_{sp}. Teflon and polytetrafluoroethylene are common solid propellant options, though these propellants have a tendency to exhibit carbon deposition which can lead to thruster failure. Ethylene tetrafluoroethylene (ETFE), Hydroxyl-terminated polybutadiene (HTPB) and Liquid perfluoropolyethers (PFPE) have been shown as possible alternatives. However ETFE exhibiting lower thrust-to-power ratio in comparison with traditional PTFE [101]. In order to investigate these new propellants properly, an understanding of the ablation process and plasma parameters is required. The power electronic circuits are also an important and integral part of PPT systems. Some recent works have focused on the implementation of solid state switching devices for the discharge capacitors which is expected to improve lifetime of PPTs. Eliminating the voltage reversal on the energy storage capacitors by using alternative circuit topologies opposed to Resistor, Inductor, Capacitor (RLC) as well as improving the efficiency with high speed, bidirectional IGBTs or MOSFETS [102]. Alternatives such as the BM topology and the pulse compression ring circuit have been proposed to enhance performance. The effect of these alternatives on the thrust, specific impulse and delta v has not been explored [102]. The use of PPTs for orbit raising would require the thrust and lifetime to be increased. Characterising the behaviour of the main energy storage capacitor over long operating times at elevated temperatures would help to improve lifetime. While adaption of circuit topologies and minimization of peripheral inductivity leads to thrust efficiencies of even more than 30% in the case of ADD SIMPLEX [99,103]. Using high Q energy storage capacitors may also help to reduce the high temperatures, as well as heat shrinks which optimise the performance over the required operating duration [102]. The adaption of the area specific energy for the propellants can lead to a minimization of charring in the long term operation and, in addition, it also can increase the thrust efficiency further as demonstrated with the coaxial (E < 10 J) PETRUS thruster [104,105]. PPTs can be easily scaled up or down in size which is highly advantageous and means that this type of EP can apply to a wider range of applications.

5.2. *Magneto-Plasma-Dynamic*

Magnetoplasmadynamic thrusters (MPD) are the most powerful of the electric thrusters [106]. Although their development typically requires rare, large and expensive vacuum test chambers [24]. They come in two types, self field and applied field. Applied field MPDs, as shown in Figures 10a and 12a, possess a magnetic field that encapsulates the exhaust, where as self field MPDs have an extended cathode. SF MPDs as shown in Figure 13, typically require very high currents to induce the self-containing magnetic field, powers in the order of 100 kW. While AF MPDs, shown in Figure 12 require much lower powers, potentially as low as 10 kW making them far more suitable to smallsats when compared with SF MPDs [106]. MPDs are similar in principle to PPT thrusters except that they use liquid propellants as opposed to generally solids in PPTs [95]. Magnetoplasmadynamic thrusters can also carry a denser plasma which cannot be achieved in many of the other types of electric propulsion as more electrons are colliding with atoms and ions, making it more difficult for them to carry the hall current [107]. The magnetoplasmadynamic thruster allows for a denser plasma by having an anode that is far greater aligned with the electric field, this reduces the amount of disruptive collisions by setting an effective anode radius to control the magnitude of the Lorentz force [107,108]. To calculate the thrust of a magnetoplasmadynamic thruster an equation has been derived where upon comparison with experimental results, the overall predicted result was acceptable [109], see Equation (18).

$$\tau = \frac{1}{2}\left(V_{z0}\sqrt{V_{z0}^2 + \omega^2 r_a^2 - \omega^8 r_a^8 \frac{R_m^3}{\alpha^3 k^6}} \cos\theta_{div} \right)\dot{m} \tag{18}$$

where V_{zo} is the velocity at the exhaust, ω is the angular velocity and is a function of the ratio between the radius of the cathode to the radius of the anode, r_a being the radius of the anode and R_m the radius of the magnetic coil. k is a detachment parameter, that predicts the critical point when particles detach from the magnetic nozzle, α is the detachment abscissa and θ_{div} is the jet divergence angle. Note that this calculation is for the case of an applied field MPD thruster.

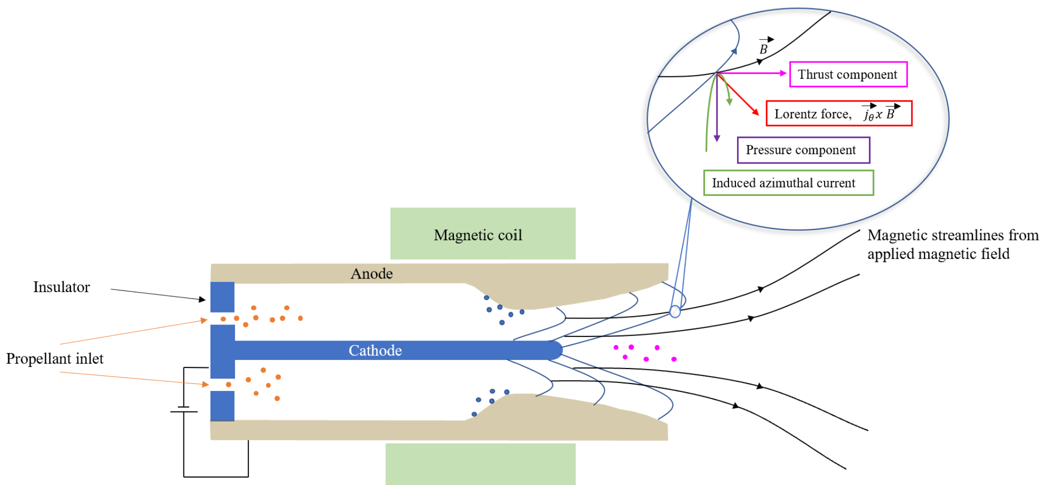

Figure 12. An Applied Field MagnetoPlasmaDynamic Thruster as a simplified schematic diagram.

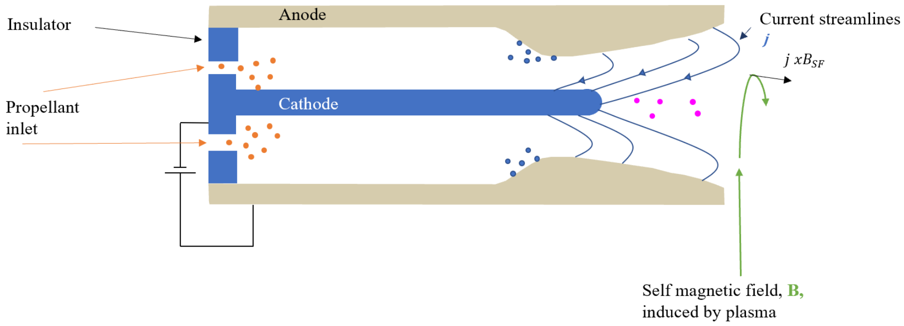

Figure 13. A Self Field MagnetoPlasmaDynamic Thruster as a simplified schematic diagram.

Recent work on MPDs attempts to reduce erosion, improve simulation environments and identify alternative propellants. There is also an increasing interest amongst the community to develop MPDs that can be utilised in CubeSats and smaller satellites. As mentioned for Hall thrusters, obtaining experimental results for thrusters which generate plasmas can be difficult. It should be noted, however, that a new method of obtaining temperature measurements and controlling the temperature for all electric thrusters, particularly magnetic thrusters has been proposed [110]. The advantage of this temperature monitoring and control system is that it can apply to all types of electric thrusters, enabling various systems to be converged into one overall propulsion system. This could be particularly useful for monitoring and controlling plasma temperatures in MPD thrusters [110] to ensure the maximum operating temperature is not exceeded. Of course, it also helps to refine the experimental findings by providing more input data. Since MPD thrusters require high power to operate, typically hundreds of kilowatts, scaling them down for smaller satellites proves to be extremely challenging. They require such high power levels because they avoid the use of grids for plasma acceleration [111], these high energies are primarily due to the plasma source, that of the ion beam. A novel method for reducing these high powers is Compact ECR Plasma Source (CEPS) developed at IIT in Delhi, this system can generate thrust values of ≈50 mN by using just 600 W of power, with a high density plasma, high bulk electron temperatures and plasma potentials [111]. This new development could help to scale these systems down for smaller satellites. Propellants for MPDs include gases such as helium, argon and hydrogen however solid propellants have been proposed [112]. The advantage of using solid propellants in these thrusters is that it removes the need for a complex propellant feed system, reducing the mass of the system. To use the solid propellant it is held in the hollow cathode tube and ignited by a laser. Igniting the propellant with a laser allows for higher ionisation of the plasma thus enabling a more stable discharge [112]. By combining both CEPS and laser ablated solid propellants into one MPD thruster, a small, lightweight CubeSat sized system can be envisioned. Other recent works have focused on erosion. Erosion on MPDs varies with the relative position of the accelerating magnetic field and typically is found on the divergent part, a reduced anode mass flow rate leading to enlarged erosion on the cathode [113]. Erosion could be reduced by an applied axial converging/diverging magnetic field at the cathode. One development which is optimised for CubeSats for example has been proposed by [114]. This could be specifically for interplanetary smallsats. Essentially, a two-stage system has been proposed [114] combining a low power micro-cathode arc thruster (μCAT) with an MPD thruster and an external magnetic field. This system is theoretically capable of orbit raising and escape of small satellites.

6. Alternative Approaches

6.1. Light Sails

A light sail is propelled by either solar radiation pressure (SRP) from the Sun, as shown in Figure 14a or theoretically from the light generated by a laser. Solar sail velocity is dependent on the distance the lightsail lies relative to a star. Hence the associated acceleration that can be achieved is proportional to the relative distance [115]. However, there are many factors which determine the final velocity of the sail. This includes sail size, reflectance properties of the sail materials, the angle at which photons strike the surface of the sail, the shape of the sail, the mass of the sail and the overall mass relative to the payload mass. Assuming an orbit around the Earth, the force our Sun puts on a solar sail is estimated using Equation (19).

$$F_{SRP} = v\frac{I}{c}(C_R)(A_s) \tag{19}$$

where I is the intensity of light calculated by the average power output (3.8×10^{26} W for the sun) divided by 4π times the distance to the source squared, alternatively, $I = P_{out}/(4\pi(S)^2)$, c is the speed of light in a vacuum, C_R is the coefficient of reflectivity of the material and A_s is the absorption area of the sail and v is simply a place holder for in shadow, 0, or not in shadow, 1. To calculate the acceleration experienced by the lightsail due to this pressure, newtons second law can simply be re-arranged for a, to give $a = F_{SRP}/m$. While light sails are still in the very early days of their realisation, many missions listing their inclusion have been proposed since the 1980s. The first successful demonstration of a light sail was by a JAXA solar sail spacecraft known as IKAROS in 2010. Since then, the Planetary society is the only other organisation to demonstrate that a spacecraft can be propelled by SRP [116]. The Planetary societies light sail 2 noted issues with power due to having only one solar panel and highlighted that atmospheric drag at 720km orbit was a significant issue [116]. These issues are expected to be addressed on the planetary societies lightsail 3. Light sails require a highly reflective material. To increase the reflectivity, the sail could be tailored to suit a specific wavelength of light to reduce absorption of photons by creating an optical barrier which prevents photons of a particular wavelength from passing through the selected material. Materials such as aerogel films were proposed by [117], however creating ultrathin aerogel films is challenging, though a flexible, freestanding, easily fabricated graphene-based aerogel film has been proposed by [118]. Some recent models of materials from an EU based research group predict that aero-graphite could offer an alternative to laser driven sail by approaching the sun at 0.4 AU with such a light material that could result in speeds of up to 6900 $\mathrm{km/s^{-1}}$ [119]. A recent demonstration of how laser light can manipulate mechanical processes of tiny optical nanomachines could be very advantageous. Potentially actuating parts of the light sail or initiating mechanical processes remotely [120]. Laser driven or beam powered propulsion, which operates over a continuous waveform (CW), is thought to offer a large reduction in cost whilst also greatly increasing the potential velocities due to a continuous acceleration and low mass ratios by not carrying the fuel. Some models estimating speeds of up to 26% the speed of light [3]. Laser-ablation systems on the other hand, which generally operate in a pulsed mode, have demonstrated potential ground to orbit laser propulsion by firing an ablative laser at a target surface of specific material and identifying optimal properties for maximum thrust [121]. No laser driven propulsion system has been demonstrated in space to date though the theoretical approach has been widely formulated and accepted. The cost to produce a laser at high power wavelengths (1.06 µm) is currently too high for interstellar missions proposed from Breakthrough Starshot, for instance. However projections estimate that laser costs will reduce significantly in the next 10 years [3]. Currently, solar sail craft have been successfully demonstrated, whereas a laser driven sail craft is yet to be technically demonstrated. A technology demonstration mission is highly desirable and could consist of a simple array of laser diodes directed at a small lightsail to propel it, this could be envisaged on the smallsat mission capability range.

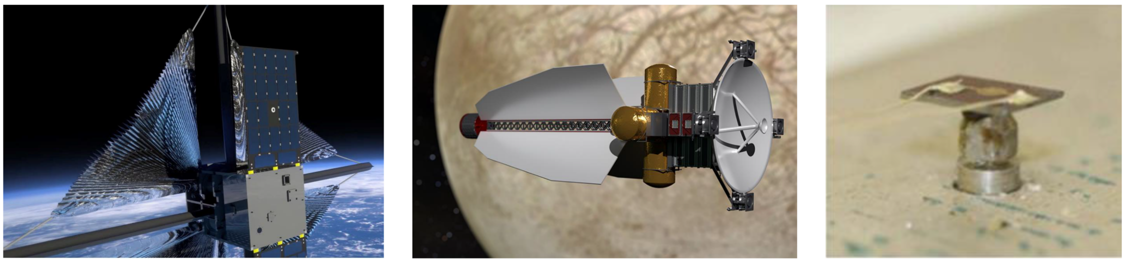

(a) (b) (c)

Figure 14. Examples of alternative approaches: (**a**) Advanced Composite Solar Sail System (ACS3), solar sail size ≈80 m^2 credits: NanoAvionics/NASA, (**b**) Swarm-Probe Enabling ATEG Reactor, or SPEAR, concept image credits: Troy Howe, and (**c**) Porous silicon thruster and sensor designed at the University of Maryland which is 2 mm total size credits: W.A. Churaman.

6.2. Nuclear

Nuclear electric propulsion (NEP) may be fission or fusion based, where fission is the splitting of an atom and fusion the combination of them. Fusion has not yet generated greater output compared to energy input, though a lot of exploratory work exists for methods and principles for how this energy may be utilised for space missions, while fission can be utilised but is still highly controversial with many safety concerns yet to be addressed [122]. Due to these concerns, most fission designs are currently only considered for deep space missions [123]. For NEP, the nuclear reactor is used to produce large amounts of electricity to propel the spacecraft, for a NEP ion thruster, specific impulses in the range of [2000–10,000] s are envisaged [124].

Fusion can be ignited but not maintained, maintaining fusion for a long enough period to allow for accelerated growth of fusion processes remains a significant challenge [125]. The energy that is initially required to ignite a fuel is largely dependant on the fuel being used and the method of ignition, it was recently shown that using a deuteron laser beam in an inertial confinement fusion reactor significantly reduced the ignition energy required for $^3He - ^3 He$ fuel [125]. The use of lasers to reduce ignition energies has also been recently demonstrated using Boron fusion whereby a high current of energetic α particles was observed [126]. Reducing the ignition energy required for fusion is therefore an important parameter that could aid the development of maintaining a fusion process with adequate output. Modelling of the plasma is clearly an important aspect of furthering research into fusion, specifically, modelling of magnetising hyper-velocity plasma jets for magnetic inertial fusion that has a target which is compressed by an imploding liner (metal target surrounding the fuel) reduces the amount of power required for fusion ignition due to the magnetic field in the target suppressing cross-field thermal conduction [127]. Other challenges with fusion include power generation, transfer and storage, thermal management and related materials [128]. Due to expanding interest and research into the expansion of humans and satellites, robots etc into space, fission is now also being reviewed as a potential energy source for space exploration [129]. Using a monte carlo simulated code in SERPENT showed that a molten salt fast reactor is a viable fission option for the nuclear-activation enhanced magnetohydrodynamic (MHD) cycle [130]. Though simulations of the non-equilibrium ionisation processes of Rb vapour within the core of the reactor is desirable to determine the viability [130]. These propulsion systems mainly apply to much larger systems in comparison to small satellites or microthrusters, however, there exists some concepts that apply to small satellites. Most commonly, radioisotope thermoelectric generators are used (RTG) [131]. These systems have generally used plutonium but plutonium is scarce and identifying alternative radioisotopes is important for future small satellite probe missions [132]. An advanced thermoelectric generator was proposed by Howe technologies whereby a power conversion system allows for the use of low enriched uranium (LEU) as the fuel source which is more widely available, though the proposed system, SPEAR as shown in Figure 14b above, only transports the

CubeSats but scaling of the system for a CubeSat is envisaged. The use of thermoelectric generators onboard CubeSats would significantly increase lifetime and mission capability. A system called Prometheus that exploits in-space temperature gradients with the use of thermoelectric modules (TEM) produced a 30 W model TEG system with a mass of 2 kg and power density of 55 W/kg [133]. A possible new method of using nuclear energy for propulsion is through ablating decay particles at a metal plate, such as alpha particles. Alpha decay is when an atomic nucleus emits an alpha particle, in theory, the emission of this particle imparts momentum, such a system using a thin filament of polonium coated with 20 µm aluminium boards, could produce thrusts of 29.5 nN/cm^2 [134], various materials and thicknesses have yet to be fully investigated along with suitable applied experimental validation procedures.

6.3. Other

There exists many potential propulsion technologies available to small satellites as well as for the purposes of interplanetary trajectories. Some of the unexplored options in this article include the nano-particle field extraction thruster (nanoFET) which provides thrust by emitting charged particles which can be varied in size and by varying the particle size this can offer a theoretical specific impulse range from 100 to 10,000 s [135]. Microwave arcjets utilise microwave energy to create a free floating plasma discharge in a microwave resonant cavity instead of using a heater element as in the case of arcjets and resistojets [136,137]. Another electrothermal propulsion system approach is the Variable Specific Impulse Magnetoplasma (VASIMR) thruster rocket, it utilises radio waves to ionise an inert propellant forming a plasma, it is then accelerated using a magnetic field. This propulsion system is largely still under development, experiments have shown continuous operating times of 2 h [138], improving the firing time of these thrusters is desirable with outgassing being the general duration limiting factor. Electrodeless thrusters use directed plasma without an anode or cathode by shaping electric or magnetic body forces to act on the propellant, this system would therefore eliminate typical ion flux and energy ablation of inner channels in electromagnetic thrusters, though extended lifetime measurements would be required to validate this [139]. Pulsed inductive thrusters also do not use an electrode, an ejection of gas is sprayed across a flat induction coil of wire where a capacitor bank releases tens of kilo volts of high voltage direct current lasting microseconds into the coil, this ionises the gas and causes charged particles to move in the opposite direction of the capacitor pulse, the plasma is then accelerated by the lorentz force out of the exhaust [140]. A helicon-double layer thruster (HDLT) injects gas into a tubular chamber with an RF antenna wrapped around the outside, the RF antenna emits electromagnetic waves causing the gas to break down and form a plasma, within the tubular chamber a magnetic field that diverges like a nozzle towards the open end accelerates the propellant [141]. This system has also been proposed for air breathing propulsion for low earth orbit satellites [142], very applicable to CubeSats since most orbit in LEO. Other newer developments for possibly the smallest scale satellites is energetic porous silicon [143] as shown in Figure 14c. This system is mainly suited to chipsats, tiny chip satellites usually weighing less than 100 g in a few cm squared, falling into the gram scale class of femtosatellites [144]. These chipsats could enable entirely new scientific missions, such as large atmospheric surveys of planets within the solar system and potentially exoplanets in the distant future due to their ability to communicate and span wide breaths across a solar system object [145]. Further improvements to these thrusters could be achieved by investigating thruster geometries [143]. An EP system which could be important for station keeping and potentially for interplanetary missions is electrodynamic tethers. An electrodynamic tether works by utilising the geomagnetic field of the Earth through the Lorentz force. It could also be used by other planets providing they have a magnetic field. It works by extending a long, conductive wire between a collector and emitter (anode and cathode) which is perpendicular to the Earth's geomagnetic field. If the anode is facing the Earth, a current will flow downwards from emitter to collector resulting in an opposing force that pushes the spacecraft higher in orbit [146]. If reversed the opposite happens and this can be used to aid safe de-orbiting. Electrodynamic tethers are propellant-less propulsion systems. They can provide station keeping and orbital maneuvering, they are re-usable, low weight and cost effective. They have been proposed as a cost effective alternative for constellation maintenance opposed to continuous replacement of whole satellites [147]. Vacuum Arc Technology (VATs) is another important and recently developed concept that should also be mentioned. If igniting an arc within a vacuum, the cathode becomes the source of the ejected material. This erodes the cathode away and becomes the means of propulsion. VATs have shown experimental specific impulses of 1000 s with µN thrust ranges [148]. The principle of VATs is akin to arcjet thrusters but they operate inside of a vacuum and the propellant is the cathode, this means no propellant feed system is required thus reducing the overall weight working towards a smaller system. Vacuum arc technology for thrusters is still in the early days of development, though initial results have been promising [149]. Most of the experimental work has yet to consider small spacecraft limitations and requirements [148] but some more recent works [149] are beginning to bridge this gap. The VAT thrusters can operate in DC or in pulsed mode but due to power and current limitations on smallsats, only pulsed VATs are practical [150]. VATs could become a more popular choice among smallsat designers due to their low power, low weight and orbit control capabilities. The technology typically requires a lower cost to implement. Finally, one of the more recent, novel and developing concepts is inertial electrostatic confinement (IEC) undergoing testing and validation at IRS in Stuttgart [151]. IEC was a fusion concept originally proposed in the 1950s and is now being investigated as an alternative plasma generation and confinement technology for EP. IEC works by applying a high voltage between two concentric spheres, one an outer anode and the other an inner cathode. This generates a plasma by the collision of electrons, emitted from the cathode, with neutral particles inside of the anode. Ions created in the process are accelerated by the electric field towards the centre of the anode. The confinement of an IEC greatly improves the plasma densities attainable and if the particles can attain high enough kinetic energies they can be extracted/accelerated out of an exhaust from the core region. This concept offers a wide degree of functionality to many different types of missions in theory and is a completely new topic within the field of EP, thus offers a lot of scope for theoretical modelling and experimental inquiry [152]. The potential experimental investigation of various gas species to optimise the plasma source as well as the suitable scaling and optimisation of the extraction nozzle would be highly desirable [151].

7. Discussion

The topic of electric propulsion systems is becoming an extremely active global research area for various research laboratories at leading Universities and Institutions as well as for commercial enterprise. One of the major challenges for electric propulsion approaches in comparison to chemical propulsion is the duration of time that it takes for the system to reach high thrust, often taking a much longer time in comparison to minutes or seconds for chemical systems. This limits electric propulsion systems to very specific in-space applications such as station keeping, collision avoidance etc. The usage of higher power systems would significantly improve the time it takes for electric propulsion systems to reach high delta v values for more timely interplanetary missions. Currently, smallsats typically orbit in LEO. The number of smallsats in LEO will be increased with the advent of micro-launchers which plan to target the smallsat market directly. Micro-launchers will reduce costs but those planned will only deliver to LEO. Once in LEO, having an adequate propulsion system to raise orbit to MEO or GEO will be highly advantageous. EP systems that can raise a smallsats orbit from LEO to MEO, GEO or beyond reduce costs further in comparison to direct launcher delivery to higher orbits. However, the drawback is that, there is a long operating time associated to these maneuvers with EP systems [6]. Enabling high thrust EP on smallsats for interplanetary probe missions would further reduce costs to solar system objects. The parameters that determine the propulsion systems ability to go interplanetary or raise orbits, avoid collisions and perform station keeping is largely dependent on how long it can last and how much thrust it can produce, i.e., its lifetime and delta v.

Lifetime suffers from space weather, ablation of propellant onto the inner wall surfaces and electro-chemical degradation along with many other aging and stress factors specific to the type of thruster. Lifetimes of smallsats can range from 10 years to under 1 year and since many space missions often operate past their expected end of life (EOL), the development of machine learning (ML) algorithms and approaches for advanced prognosis and diagnosis of the electric thruster subcomponents will become more important going forward. This would improve the robustness and reliability and enable accurate estimation of the remaining useful lifetime (RUL), all of which, will work towards increasing the longevity. This could be achieved by using accelerated aging test-beds to gather prognostics data to characterise the state of health of the thruster and subsystems. This data could then be used to model the degradation and apply ML algorithms for advanced prognostics and condition based monitoring (CbM) of the thruster. Robustness of electric propulsion systems for missions beyond Earth orbit is critical for future, longer missions.

Additive Manufacturing (AM) processes could also greatly improve the lifetime of thruster systems as well as other important design performance and optimisation aspects. The traditional methods of manufacturing parts for these propulsion systems such as welding, CNC machining and injection molding contain more procedures and require more parts in comparison to AM. Identifying optimal AM processes and materials to increase the max temperature of the ohmic heater in electrothermal thrusters could provide them with much higher exhaust velocities. Using AM for the production of Taylor cones in electrospray thrusters offers the potential to explore many different array layouts, processes and configurations for optimised design. Smallsat mass can also greatly benefit from additive manufacturing techniques. 3D printed carbon fibre frames, advanced composites and metamaterials could greatly reduce the mass and increase the potential delta velocities attainable.

The choice of electric propulsion system is distinguished by the scientific objectives of a specified mission. Traditionally, 62% of operational missions used resistojets with 34% choosing hall thrusters [15]. For smallsats under 50 kg, 38% have used electrospray thrusters and 33% have used pulsed plasma thrusters. Currently, no single thruster can achieve a wide array of manoeuvrability, specific impulse, continuous acceleration, lifetime and adequate thrust efficiency and sensitivity for a range of smallsat requirements. Although many EP systems such as the PPT, arcjets and electrosprays are easily adaptable and can be scaled to various missions with specific mass, power and payload budgets. While EP systems that are less adaptable such as SF MPDs, NEP and resistojets are more suitable to missions with specific purpose. Capability demonstration is therefore an important aspect to proof the various EP systems. For example, demonstrating the capability of the smallest available satellites to the scientific community, femtosats, offers the potential to increase interest and adoption of these platforms for space missions. Surveying the sensor capability of femto-satellites with EP systems would enable a broader community to consider the potential scientific findings they can contribute towards. Specifically by outlining payload capability vs delta v and propellant mass trade-offs. As mission payloads increase, delta v capability decreases [22]. Still, by equipping such small satellites with propulsion systems, the range of scientific objectives increases and therefore so too does the demand and interest levels. An arising issue however, is the complex testing facilities needed on the ground to validate these EP systems, as promising ground performances does not always correspond to promising in-space performance [19]. Mass is a critical factor when designing smallsats and considering which EP system to include raises many design trade-off options to consider. The average mass of smallsats launched into orbit is currently 109 kg with a 6 times increase since 2017 and 2 times increase since 2018 [153]. Mass and cost budgets and mission objectives largely determines the EP system chosen. For example, EP systems proposed for station keeping typically include PPTs, resistojets, arcjets and electrosprays. Station keeping will be an important parameter for future smallsats as more enter orbit but even more so will be collision avoidance considering space debris. Collision avoidance would typically require high delta velocities depending on the notice period before a collision occurs. This would favour those EP systems that can therefore provide higher thrust forces, although if sufficient notice is given, most EP systems could avoid the collision. Orbit raising will require high thrust and long lifetime EP systems. Considering the mass and power budgets of smallsats most EP systems are not currently suited to orbit raising although they are gradually becoming more capable in this direction.

The associated electronics and power for small satellites plays an important role in determining the propulsion system. The average power range for satellites is in constant growth. Electromagnetic systems depend heavily on highly efficient power supplies with SF MPDs typically requiring more than 100 kW of power to operate various magnetic and electric fields whilst also ionising the plasma. The use of Thermo-Electric Generators (TEGs) for smallsats as a power source for higher power propulsion systems such as the AF MPD thruster could enable far broader mission capabilities [133]. Determining the relationship between thrust performances and the selection of circuit topologies within the power supply and associated circuits has great potential to improve the efficiency thus improving overall delta v and the systems longevity. The development of compact, safe and efficient power supply systems is important for the advancement of these technologies [19]. The growth of the smallsat and 'new space' industry requires EP systems that can accurately, sensitively and adequately maneuver objects in space. Moreover, highly efficient, high thrust, low cost EP systems have the potential to advance scientific studies into the solar system for the expansion of our knowledge and understanding. While a vast array of different EP concepts and approaches exists, however they are generally limited to specific missions or objectives. Current systems are not able to perform all of the required tasks such as avoid collisions, raise orbits, station keeping, de-orbit appropriately or achieve interplanetary trajectories. As they are severely limited to specific orbits, mission parameters and agreed upon lifetimes. It would be valuable to have EP systems that enable more options and opportunities for high value smallsats past their expected EOL instead of cluttering up in LEO until they de-orbit. There is a need for on-orbit servicing to avoid high value products being simply disposed of once they meet their EOL. Supplied with adequate EP systems, smallsats could provide more ambitious mission objectives, scientific gains and achievements.

8. Conclusions

For smallsats to independently escape Earths orbit, GIT, Arcjets, AF MPDs, HT, Resistojets, Electrospray, VATs and Light sails are identified as the most promising propulsion systems. If improvements to the thrust and specific impulse, nozzle geometries, lifetime, power demands and propellant efficiency can be made to SF MPDs, PPTs, Porous Silicon based, NEP, VASIMR and HDLT thrusters, then these should be considered for smallsat interplanetary missions. The current landscape of electric space propulsion has been reviewed covering the four thematic areas of electrostatic, electrothermal, electromagnetic and alternative approaches. Limitations and shortcomings of existing EP systems have also been presented and discussed, as well highlighting potential research avenues, approaches to advance the wider field. Hence, our future work will be heavily informed by these findings and will thus focus on some of the areas identified in this paper to increase the performance, efficiency as well as robustness of the systems. All of which will work towards increasing the knowledge base around the core EP technologies for smallsat systems for novel interplanetary missions.

Author Contributions: Conceptualization, D.O., G.H. and D.F.K.; methodology, D.O. and D.F.K.; software, D.O. and D.F.K.; validation, D.O. and D.F.K.; formal analysis, D.O., G.H. and D.F.K.; investigation, D.O., G.H. and D.F.K.; resources, D.O. and D.F.K.; data curation, D.O. and D.F.K.; writing—original draft preparation, D.O.; writing—review and editing, D.O., G.H. and D.F.K.; visualization, D.O. and D.F.K.; supervision, G.H. and D.F.K.; project administration, D.F.K.; funding acquisition, D.O. and D.F.K. All authors have read and agreed to the published version of the manuscript.

Funding: This research was funded by the Irish Research Council, grant number GOIPG/2020/1566.

Acknowledgments: We would like to acknowledge support from Simon Pete Worden of the Breakthrough Initiatives for providing guidance and advice. Pete Klupar of the Breakthrough Initiatives for technical suggestions. Stephen Scully from the Institute of Technology, Carlow for fruitful discussions. Eoghan Chelmiah from the Institute of Technology, Carlow for guidance on table formatting. Martin Tajmar from Dresden University for guidance.

Conflicts of Interest: The authors declare no conflict of interest. The funders had no role in the design of the study; in the collection, analyses, or interpretation of data; in the writing of the manuscript, or in the decision to publish the results.

Abbreviations

The following abbreviations are used in this manuscript:

AM	Additive Manufacturing
ALM	Additive Layer Manufacturing
BM	Bidirectional Mosfet
CAT	Micro Cathode Arc Thruster
CEPS	Compact ECR Plasma Source
CGS	Cold Gas Thrusters
CNC	Computer Numerical Control
DAB	Dual Active Bridge
DART	Double Asteroid Redirection Test
EOL	End of Life
EP	Electric Propulsion
ESU	Energy Storage Unit
ETFE	Ethylene Tetrafluoroethylene
FFEP	Field Emission Electric Propulsion
GEO	Geostationary Earth Orbit
GIT	Gridded Ion Thruster
HET	Hall Effect Thruster
HTPB	Hydroxl-terminated polybutadiene
IGBT	Insulated Gate Bi-Polar Transistor
LEO	Low Earth Orbit
LRP	Laser Radiation Pressure
LPM	Low Power Micro-Resistojet
MEO	Middle Earth Orbit
ML	Machine Learning
MPD	Magnetoplasmadynamic
TAL	Thruster with Anode Layer
PPT	Pulsed Plasma Thruster
PFPE	Liquid perfluoropolyethers
PPU	Power Processing Unit
RLC	Resistor, Inductor, Capacitor
RUL	Remaining Useful Lifetime
SLS	Space Launch System
SPT	Stationary Plasma Thruster
STAR	Super High Temperature Additive Resistojet
TEG	Thermal Electric Generator
VAT	Vacuum Arc Thruster

References

1. Krejci, D.; Lozano, P. Space Propulsion Technology for Small Spacecraft. *IEEE Xplore* **2018**, *106*, 362–376. [CrossRef]
2. Staehle, R.L.; Anderson, B.; Betts, B.; Blaney, D.; Chow, C.; Friedman, L.; Hemmati, H.; Jones, D.; Klesh, A.; Liewer, P.; et al. Interplanetary CubeSats: Opening the Solar System to a Broad Community at Lower Cost. *JoSS* **2012**, *2*, 161–186. Available online: https://jossonline.com/Papers1441.html (accessed on 2 October 2020).
3. Lubin, P. A Roadmap to Interstellar Flight. *JBIS* **2016**, *69*, 40–72. Available online: https://www.jbis.org.uk/paper/2016.69.40 (accessed on 4 October 2020).
4. Levchenko, I.; Xu, S.; Teel, G.; Mariotti, D.; Walker, M.L.R.; Keidar, M. Recent Progress and perspectives of space electric propulsion systems based on smart nanomaterials. *Nat. Commun.* **2018**, *9*, 1–10. [CrossRef] [PubMed]
5. Levchenko, I.; Xu, S.; Mazouffre, S.; Lev, D.; Pedrini, D.; Goebel, D.; Garrigues, L.; Taccogna, F.; Bazaka, K. Perspectives, frontiers, and new horizons for plasma-based space electric propulsion. *Phys. Plasmas* **2020**, *27*, 1–18. [CrossRef]
6. Lev, D.R.; Emsellem, G.D.; Hallock, A.K. The Rise of the Electric Age for Satellite Propulsion. *New Space* **2017**, *5*, 4–14. [CrossRef]
7. Kramer, A.; Bangert, P.; Schilling, K. UWE-4: First Electric Propulsion on a 1U CubeSat—In-Orbit Experiments and Characterization. *Aerospace* **2020**, *7*, 98. [CrossRef]
8. Bonnal, C.; Phipps, D.M.C.; Dupont, C.; Missonnier, S.; Lequette, L.; Merle, M.; Rommelaere, S. Just in time collision avoidance – A review. *Acta Astronaut.* **2020**, *170*, 637–651. [CrossRef]
9. Levchenko, I.; Keidar, M.; Cantrell, J.; Wu, Y.L.; Kuninaka, H.; Bazaka, K.; Xu, S. Explore space using swarms of tiny satellites. *Nature* **2018**, *562*, 185–187. [CrossRef]
10. Racca, G.; Marina, A.; Stagnaro, L. SMART-1 mission description and development status. *Planet. Space Sci.* **2002**, *50*, 1323–1337. [CrossRef]
11. Sternberg, D.; Sternberg, D.; Essmiller, J.; Colley, C.; Klesh, A.; Krajewski, J. Attitude Control System for the Mars Cube One Spacecraft. In Proceedings of the 2019 IEEE Aerospace Conference, Big Sky, MT, USA, 2–9 March 2019; pp. 1–10. [CrossRef]
12. Block, D.J.; Astrom, K.J.; Spong, M.W. The Reaction Wheel Pendulum. *Synth. Lect. Control Mech.* **2007**. [CrossRef]
13. Malphrus, B.K.; Freeman, A.; Staehle, R.; Klesh, A.T.; Walk, R. 4 - Interplanetary CubeSat missions. *Cubesat Handb. Mission Des. Oper.* **2021**, *1*, 85–111. [CrossRef]
14. Tummala, A.R.; Dutta, A. An Overview of Cube-Satellite Propulsion Technologies and Trends. *Aerospace* **2017**, *4*, 5–26. [CrossRef]
15. Lev, D.; Myers, R.; Lemmer, K.; Kolbeck, J.; Koizumi, H.; Polzin, K. The technological and commercial expansion of electric propulsion. *Acta Astronaut.* **2019**, *159*, 213–227. [CrossRef]
16. Hudson, J.; Spangelo, S.; Hine, A.; Kolosa, D.; Lemmer, K. Mission Analysis for CubeSats with Micro propulsion. *Spacecr. Rocket.* **2016**, *53*, 5. [CrossRef]
17. McDowell, J.C. The Low Earth Orbit Satellite Population and Impacts of the SpaceX Starlink Constellation. *Astrophys. J. Lett.* **2020**, *892*, 1. [CrossRef]
18. Levchenko, I.; Xu, S.; Wu, Y.; Bazaka, K. Hopes and concerns for astronomy of satellite constellations. *Nat. Astron.* **2020**, *4*, 1012–1014. [CrossRef]
19. Levchenko, I.; Bazaka, K.; Ding, Y.; Raitses, Y.; Mazouffre, S.; Henning, T.; Klar, P.J.; Shinohara, S.; Schein, J.; Garrigues, L.; et al. Space micropropulsion systems for Cubesats and small satellites: From proximate targets to furthermost frontiers. *Appl. Phys. Rev.* **2018**, *5*, 011104. [CrossRef]
20. Messerschmitt, D.G.; Lubin, P.; Morrison, I. Challenges in Scientific Data Communication from Low-mass Interstellar Probes. *Astrophys. J.* **2020**, *249*, 2–10. [CrossRef]
21. Turner, M.J. *Rocket and Spacecraft Propulsion*; Astronautical Engineering Springer: Berlin/Heidelberg, Germany, 2006; pp. 14–17. [CrossRef]
22. Conversano Ryan, W.; Wirz Richard, E. Mission Capability Assessment of CubeSats Using a Miniature Ion Thruster. *J. Spacecr. Rocket.* **2013**, *50*, 1036–1037. [CrossRef]
23. Spangelo, S.; Dalle, D.; Longmier, B. Integrated Vehicle and Trajectory Design of Small Spacecraft with Electric Propulsion for Earth and Interplanetary Missions. In Proceedings of the 29th Annual AIAA/USUConference on Small Satellites, Logan, UT, USA, 8–13 August 2015; pp. 1–16.
24. Mazouffre, S. Electric propulsion for satellites and spacecraft: Established technologies and novel approaches. *Plasma Sources Sci. Technol.* **2016**, *25*, 033002. [CrossRef]
25. Liu, B.; Li, X.; Yang, J.; Gao, G. Recent Advances in MEMS-Based Microthrusters. *Aerospace* **2019**, *10*, 818. [CrossRef] [PubMed]
26. Thuppul, A.; Wright, P.L.; Collins, A.L.; Ziemer, J.K.; Wirz, R.E. Lifetime Considerations for Electrospray Thrusters. *Aerospace* **2020**, *7*, 108. [CrossRef]
27. Krejci, D.; Mier-Hicks, F.; Thomas, R.; Haag, T.; Lozano, P. Emission Characteristics of Passively Fed Electrospray Microthrusters with Propellant Reservoirs. *J. Spacecr. Rocket.* **2017**, *54*, 447–458. [CrossRef]
28. Guerra-Garcia, C.; Krejci, D.; Lozano, P. Spatial uniformity of the current emitted by an array of passively fed electrospray porous emitters. *J. Phys. D Appl. Phys.* **2016**, *49*, 1. [CrossRef]
29. Tsay, M.; Model, J.; Barcroft, C.; Frongillo, J.; Zwahlen, J.; Feng, C. Integrated Testing of Iodine BIT-3 RF Ion Propulsion System for 6U CubeSat Applications. In Proceedings of the 35th International Electric Propulsion Conference Georgia Institute of Technology, Atlanta, GA, USA, 8–12 October 2017; p. 1.

30. Demmons, N.; Hruby, V.; Spence, D.; Roy, T.; Ehrbar, E.; Zwahlen, J.; Martin, R.; Ziemer, J.; Randolph, T. ST7-DRS Mission Colloid Thruster Development. In Proceedings of the 44th AIAA/ASME/SAE/ASEE Joint Propulsion Conference & Exhibit, Hartford, CT, USA, 21–23 July 2008. [CrossRef]
31. Chengyu, M.; Charles N, R. The Design and Characterization of a Porous-emitter Electrospray Thruster (PET-100) for Interplanetary CubeSats. In Proceedings of the 7th Interplanetary Cubesat Workshop, Paris, France, 29–30 May 2018; p. 1. Available online: https://icubesat.org/wp-content/uploads/2018/06/b-2-3-201805301309-paper.pdf (accessed on 23 October 2020).
32. Bretti, M. AIS-ILIS1 Ionic Liquid Ion Source Electrospray Thruster. Applied Ion Systems LLC. 2020. Available online: https://appliedionsystems.com/portfolio/ais-ilis1-ionic-liquid-ion-source-electrospray-thruster/ (accessed on 2 November 2020).
33. Koppel, C.R.; Marchandise, F.; Prioul, M.; Estublier, D.; Darnon, F. The SMART-1 Hall Effect Thruster Around the Moon: In Flight Experience. In Proceedings of the 41st AIAA/ASME/SAE/ASEE Joint Propulsion Conference & Exhibit, Tucson, AZ, USA, 10–13 July 2005. [CrossRef]
34. Vaudolon, J.; Vial, V.; Cornu, N.; Habbassi, I. PPSR©X00 Thruster Development Status at Safran. In Proceedings of the 36th International Electric Propulsion Conference,Vienna, Austria, 15–20 September 2019. Available online: https://www.cheops-h2020.eu/wp/wp-content/uploads/IEPC-2019-241_SAFRAN_Vaudolon.pdf (accessed on 23 October 2020).
35. Saevets, P.; Semenenko, D.; Albertoni, R.; Scremin, G. Development of a Long-Life Low-Power Hall Thruster. In Proceedings of the 35th International Electric Propulsion Conference, Atlanta, GA, USA, 8–12 October 2017; p. 2.
36. Misuri, T.; Ducci, C.; Gregucci, S.; Pedrini, D.; Cannelli, F.; Cesari, U.; Nania, F.; Vicini, A.; Pace, G.; Magistro, F.; et al. Recent Advances in Low-Current Hollow Cathodes at SITAEL. In Proceedings of the 36th International Electric Propulsion Conference, Vienna, Austria, 15–20 September 2019; p. 8.
37. Brophy John, R. NASA's Deep Space 1 ion engine (plenary). *Rev. Sci. Instruments* **2002**, *73*, 1075. [CrossRef]
38. Szabo, J.; Pote, B.; Paintal, S.; Robin, M.; Hillier, A.; Branam, R.D.; Huffmann, R.E. Performance Evaluation of an Iodine-Vapor Hall Thruster. *J. Propuls. Power* **2012**, *28*, 848–857. [CrossRef]
39. Wirz, R.; Sullivan, R.; Przybylowski, J.; Silva, M. Hollow Cathode and Low-Thrust Extraction Grid Analysisfor a Miniature Ion Thruster. *Int. J. Plasma Sci. Eng.* **2008**, *2008*, 693825. [CrossRef]
40. Ziemer, J.; Merkowitz, S. Microthrust Propulsion for the LISA Mission. In Proceedings of the 40th AIAA/ASME/SAE/ASEE Joint Propulsion Conference and Exhibit, Fort Lauderdale, FL, USA, 11–14 July 2004. [CrossRef]
41. Thuppul, A.; Wright, P.; Wirz, R.E. Lifetime Considerations and Estimation for Electrospray Thrusters. In Proceedings of the 2018 Joint Propulsion Conference, Cincinnati, OH, USA, 9–11 July 2018. [CrossRef]
42. Krejci, D.; Mier-Hicks, F.; Fucetola, C.; Lozano, P. Design and Characterization of a Scalable ion Electrospray Propulsion System. In Proceedings of the 34th International Electric Propulsion Conference and 6th Nano-satellite Symposium, Hyogo-Kobe, Japan, 4–10 July 2015.
43. A.Jorns, B.; Gorodetsky, A.; Lasky, I.; Kimber, A.; Dahl, P. Uncertainty Quantification of Electrospray Thruster Array Lifetime. In Proceedings of the 36th International Electric Propulsion Conference, Vienna, Austria, 15–20 September 2019.
44. Huh, H.; Wirz, R.E. Numerical Simulation of Electrospray Thruster Extraction. In Proceedings of the 36th International Electric Propulsion Conference, Vienna, Austria, 15–20 September 2019.
45. Ziemer, J.; Marrese-Reading, C.; Dunn, C. Colloid Microthruster Flight Performance Results from Space Technology 7 Disturbance Reduction System. In Proceedings of the The 35th International Electric Propulsion Conference, Atlanta, GA, USA, 8–12 October 2017.
46. Block, D.; Tajmar, M. Highly miniaturized FEEP propulsion system (NanoFEEP) for attitude and orbit control of CubeSats. *Acta Astronaut.* **2018**, *144*, 422–428. [CrossRef]
47. Dale, E.; Jorns, B.; Gallimore, A. Future Directions for Electric Propulsion Research. *Aerospace* **2020**, *7*, 16–23. [CrossRef]
48. Akhmetzhanov, R.; Bogatyi, A.V.; Kashirin, D.A.; Obukhov, V.A.; Popov, G.A.; Svotina, V.V.; Khartov, S.A Low-Power Ion Thrusters. State of Development at Research Institute of Applied Mechanics and Electrodynamics, MAI. *Mater. Sci. Eng.* **2020**, *927*, 1–5. [CrossRef]
49. Dietz, P.; Gärtner, W.; Koch, Q.; Köhler, P.E.; Teng, Y.; Schreiner, P.R.; Holste, K.; Klar, P.J. Molecular propellants for ion thrusters. *Plasma Sources Sci. Technol.* **2019**, *28*, 084001. [CrossRef]
50. Bekemans, M.; Bronchart, F.; Scalais, T.; Franke, A. Configurable High Voltage Power Supply for Full Electric Propulsion Spacecraft. In Proceedings of the 2019 European Space Power Conference, Juan-les-Pins, France, France, 30 September–4 October 2019. [CrossRef]
51. Bontempo, J.J.; Brigeman, A.N.; Fain, H.B.; Gonzalez, M.C.; Birchenough, L.R.P.A.G.; Aulisio, M.V.; Fisher, J.; Ferraiuolo, B. The NEXT-C Power Processing Unit: Lessons Learned from the Design, Build, and Test of the NEXT-C PPU for APL's DART Mission. In Proceedings of the AIAA Propulsion and Energy 2020 Forum, Virtual Event, 24–28 August 2020. [CrossRef]
52. Yuan, T.; Ren, J.; Zhang, J.Z.Z.; Wang, Y.; Tang, H. The effects of numerical acceleration techniques on PIC-MCC simulations of ion thrusters. *AIP Adv.* **2020**, *10*, 045115. [CrossRef]
53. Lozano, P.; Krejci, D.; Jia-Richards, O. Staging of Ion Propulsion Thrusters. International Patent Application ID PCT/US2019/053784, 30 September 2019.
54. Krejci, D.; Jenkins, M.G.; Lozano, P. Staging of electric propulsion systems: Enabling an interplanetary Cubesat. *Acta Astronaut.* **2019**, *160*, 175–182. [CrossRef]
55. Rafalskyi, D.; Aanesland, A. A Neutralizer-Free Gridded Ion Thruster Embedded Into A 1U Cubesat Module. In Proceedings of the 35th International Electric Propulsion Conference, Atlanta, GA, USA, 8–12 October 2017.

56. Yang, J.; Jia, S.; ZHANG, Z.; Zhang, X.; LI, T.J.L.; Cai, Y.; Cai, J. Performance of a 4-cm iodine-fueled radio frequency ion thruster. *Plasma Sci. Technol.* **2020**, *22*, 094006. [CrossRef]
57. Nakagawa, Y.; Koizumi, H.; Kawahara, H.; Komurasaki, K. Performance characterization of a miniature microwave discharge ion thruster operated with water. *Acta Astronaut.* **2019**, *157*, 294–299. [CrossRef]
58. Hall, E. On a new action of the magnet on electric currents. *Am. J. Math.* **1879**, *2*, 287–292. [CrossRef]
59. Goebel, D.M.; Katz, I. *Fundamentals of Electric Propulsion: Ion and Hall Thrusters*; John Wiley & Sons Publishing: Hoboken, NJ, USA, 2008. [CrossRef]
60. Choueiri, E.Y. Fundamental Difference between the Two Variants of Hall Thrusters: SPT and TAL. In Proceedings of the 37th Joint Propulsion Conference and Exhibit, Salt Lake City, UT, USA, 8–11 July 2001. [CrossRef]
61. Shcherbanev, V.D.S.; Charoy, T.; Clément, N.; Deltel, C.; Richard, P.; Vincent, S.; Chabert, P.; Bourdon, A. Fast Camera Analysis of Plasma Instabilities in Hall Effect Thrusters Using a POD Method under Different Operating Regimes. *Aerospace* **2020**, *11*, 518. [CrossRef]
62. Greve, C.; Thomas, A.; Majji, M.; Hara, K. Real-time Estimation of Electron Dynamics in Hall Effect Thrusters using an Extended Kalman Filter. In Proceedings of the AIAA Propulsion and Energy 2020 Forum, Virtual Event, 24–28 August 2020. [CrossRef]
63. Brown, N.P.; Walker, M.L.R. Review of Plasma-Induced Hall Thruster Erosion. *Appl. Sci.* **2020**, *10*, 3–7. [CrossRef]
64. Taccogna, F.; Garrigues, L. Latest Progress in Hall Thrusters Plasma Modelling. *Rev. Mod. Plasma Phys.* **2019**, *3*, 1–52. [CrossRef]
65. Boeuf, J.P. Physics and modelling of Hall thrusters. *J. Appl. Phys.* **2017**, *121*, 011101. [CrossRef]
66. Kinefuchi, K.; Cho, S.; Fukatsu, T.; Tsukizaki, R.; Funaki, I.; Hirano, Y.; Tashiro, Y.; Shiiki, T. Keeper Ignition and Discharge Characteristics of Hollow Cathode Center-Mounted on Hall Thruster. *Propuls. Power* **2020**, *876*, 1–8. [CrossRef]
67. Lev, D.R.; Mikellides, I.G.; Pedrini, D.; Goebel, D.M.; Jorns, B.A.; McDonald, M.S. Recent progress in research and development of hollow cathodes for electric propulsion. *Rev. Mod. Plasma Phys.* **2019**, *3*, 6. [CrossRef]
68. Becatti, G.; W.Conversano, R.; M.Goebel, D. Demonstration of 25,000 ignitions on a proto-flight compact heaterless lanthanum hexaboride hollow cathode. *Acta Astronaut.* **2020**, *178*, 181–191. [CrossRef]
69. Mazouffre, S.; Tsikata, S.; Vaudolon, J. Development and experimental characterisation of a wall-less Hall thruster. *J. Appl. Phys.* **2014**, *116*, 3–10. [CrossRef]
70. Gildea, S.R.; Matlock, T.S.; Martínez-Sánchez, M.; Hargus, W.A., Jr. Erosion Measurements in a Low-Power Cusped-Field Plasma Thruster. *Propuls. Power* **2013**, *29*, 906–917. [CrossRef]
71. Dragnea, H.C.; Ortega, A.L.; Kamhawi, H.; Boyd, I.D. Simulation of a Hall Effect Thruster Using Krypton Propellant. *Propuls. Power* **2020**, *36*, 1–8. [CrossRef]
72. Kamhawi, H. Performance Evaluation of the NASA-300M 20 kW Hall Thruster. In Proceedings of the 47th AIAA/ASME/SAE/ASEE Joint Propulsion Conference & Exhibit, San Diego, CA, USA, 31 July–3 August 2011.
73. Blinov, V.; Vavilov, I.S.; Fedynin, V.V.; Shalay, V.V.; Yachmenev, P.S.; Ruban, V.I. Experimental investigations of nitrogen arcjet thruster with control unit for small spacecrafts. *J. Phys.* **2019**, *1210*, 1–6. [CrossRef]
74. Wollenhaupt, B.; Le, Q.H.; Herdrich, G. Overview of thermal arcjet thruster development. *Aircr. Eng. Aerosp. Technol.* **2018**, *90*, 280–301. [CrossRef]
75. Vavilov, I.; Fedynin, V.V.; Yachmenev, P.S.; Zharikov, K.I.; Lukyanchik, A.I.; Stepen, P.V. Review of electric thrusters with low consumption power for corrective propulsion system of small space vehicles. *J. Phys.* **2020**, *1546*, 1–10. [CrossRef]
76. Tang, H.B.; Zhang, X.A.; Liu, Y.; Wang, H.X. Numerical and Experimental Study of a 1-kW Hydrazine Engineering Design Model Arcjet Thruster. *J. Aerosp. Eng.* **2014**, *27*, 16–23. [CrossRef]
77. Zube, D.; Fye, D.; Masuda, I.; Gotoh, Y. Low bus voltage hydrazine arcjet system for geostationary satellites. In Proceedings of the 34th AIAA/ASME/SAE/ASEE Joint Propulsion Conference and Exhibit, Cleveland, OH, USA, 13–15 July 1998. [CrossRef]
78. Dropmann, M.; Ehresmann, M.; Pagan, A.S.; Le, Q.H.; Romano, F.; Montag, C.; Herdrich, G. Low Power Arcjet Application for End of Life Satellite Servicing. In Proceedings of the 7th European Conference on Space Debri, Darmstadt, Germany, 18–21 April 2017. Available online: http://spacedebris2017.sdo.esoc.esa.int (accessed on October 17 2020).
79. Herdrich, G.; Bauder, U.; Boxberger, A.; Eichhorn, C.; Lau, M.; Pfeiffer, M.; Stindl, T.; Syring, C.; Wollenhaupt, B.; Röser, H.P.; et al. Overview on Electric Propulsion Development at IRS. In Proceedings of the 32nd International Electric Propulsion Conference, Wiesbaden, Germany, 11–15 September 2011.
80. Lee, R.; Lilly, T.; Muntz, E.; Ketsdever, A. Free Molecule Micro-Resistojet: Nanosatellite Propulsion. In Proceedings of the 41st AIAA/ASME/SAE/ASEE Joint Propulsion Conference & Exhibit, Tucson, AZ, USA, 10–13 July 2005. [CrossRef]
81. Asakawa, J.; Koizumi, H.; Nishii, K.; Takeda, N.; Murohara, M.; Funase, R.; Komurasaki, K. Fundamental Ground Experiment of a Water Resistojet Propulsion System: AQUARIUS Installed on a 6U CubeSat: EQUULEUS. *Trans. Jpn. Soc. Aeronaut. Space Sci. Aerosp. Technol. Jpn.* **2018**, *16*, 427–431. [CrossRef]
82. Romei, F.; Grubišić, A.; Lasagna, D.; Gibbon, D. Multiphysics Model Validation of Resistojets with Concentric Tubular Heat Exchanger. In Proceedings of the 7th European Conference for Aeronautics and Space Science, Milan, Italy, 4–7 December 2017; pp. 1–10. [CrossRef]
83. Wollenhaupt, B.L.; A., H.; G., H.; S., F.; Röser, H.P. A Very Low Power Arcjet (VELARC) for Small Satellite Missions. In Proceedings of the 32nd International Electric Propulsion Conference, Wiesbaden, Germany, 11–15 September 2011.
84. Shen, Y.; Tong, Y.; wei, F.; yao, Z.; HU, D. Influences of characteristic parameters on starting-up process of an arcjet thruster. *Chin. J. Aeronaut.* **2020**, *34*, 7. [CrossRef]

85. Kaminska, A.; Bialek, A.; Dudeck, M. Performances of an argon arc-jet thruster for satellites. *J. Phys.* **2014**, *60*, 549–559. Available online: http://www.nipne.ro/rjp/2015_60_3-4/RomJPhys.60.p549.pdf (accessed on 12 October 2020).
86. Skalden, J.; Herdrich, G.; Ehresmann, M.; Fasoulas, S. Development Progress of an Adaptable Deorbit System for Satellite Constellations. In Proceedings of the 36th International Electric Propulsion Conference, Vienna, Austria, 15–20 September 2019.
87. Rovey, J.L.; Lyne, C.T.; Mundahl, A.J.; Rasmont, N.; Glascock, M.S.; Wainwright, M.J.; Berg, S.P. Review of multimode space propulsion. *Prog. Aerosp. Sci.* **2020**, *118*, 2–10. [CrossRef]
88. Cervone, A.; Zandbergen, B.; Guerrieri, D. Green micro-resistojet research at Delft University of Technology: new options for Cubesat propulsion. *CEAS Space J.* **2017**, *9*, 111–125. [CrossRef]
89. Evans, M.E.; Graham, D.L. A Flexible Lunar Architecture for Exploration (FLARE) supporting NASA's Artemis Program. *Acta Astronaut.* **2016**, *177*, 351–372. [CrossRef]
90. Koizumi, H.; Asakawa, J.; Nakagawa, Y.; Nishii, K.; Takao, Y.; Nakano, M.; Funase, R. Assessment of Micropropulsion System Unifying Water Ion Thrusters and Water Resistojet Thrusters. *Spacecr. Rocket.* **2019**, *56*, 2–7. [CrossRef]
91. Kim, H.S.; Young-Shin, L. Optimization design technique for reduction of sloshing by evolutionary methods. *Mech. Sci. Technol.* **2007**, *22*, 25–33. [CrossRef]
92. F.Romei.; A.N.Grubišić. Validation of an additively manufactured resistojet through experimental and computational analysis. *Acta Astronaut.* **2017**, *167*, 14–22. [CrossRef]
93. Woodruff, C. Monofilament Vaporization Propulsion Systems. U.S. Patent Application 10,724,480, 28 July 2020.
94. Webber, C.R. *Plasma, Ion-Thrusters, and VASIMR*; ASEN 5053; University of Colorado Boulder: Boulder, CO, USA, 2011; pp. 1–9.
95. MITOpenCourseWare2015. *Plasma Accelerators/Magnetoplasmadynamic (MPD)Thrusters*; Massachusetts Institute of Technology: Cambridge, MA, USA, 2015; pp. 1–14.
96. Antropov, N.; Bogaty, A.; Boykachev, V. Development of Russian Next-generation Ablative Pulsed Plasma Thrusters. *Procedia Eng.* **2017**, *185*, 56. [CrossRef]
97. Montag, C.; Burghaus, H.; Herdrich, G.; Schönherr, T. Developmemnt of a new pulsed plasma thruster and a brief introduction of a planned test facility. In Proceedings of the 67th International Astronautical Congress, Guadalajara, Mexico, 26–30 September 2016.
98. Herdrich, G.; T.Binder.; Boxberger, A.; Chadwick, A.; Chan, Y.A.; Ehresmann, M.; Harmansa, N.; Montag, C.; Romano, F.; Skalden, J.; Fasoulas, S. Research and Development on Electric and Advanced Propulsion at IRS. In Proceedings of the 35th International Electric Propulsion Conference, Atlanta, GA, USA, 8–12 October 2017; p. 4.
99. Lau, M.; Herdrich, G. Pulsed Plasma Thruster Endurance Operation Stress Testing at IRS. In Proceedings of the 33rd International Electric Propulsion Conference, Washington, DC, USA, 6–10 October 2013.
100. Chan, Y.A.; Montag, C.; Herdrich, G.; Schönherr, T. Review of Thermal Pulsed Plasma Thruster-Design, Characterisation, and Application. In Proceedings of the 34th International Electric Propulsion Conference and 6th Nano-satellite Symposium, Hyogo-Kobe, Japan, 4–10 July 2015.
101. Ling, W.Y.L.; Zhang, S.; Fu, H.; Huang, M.; Quansah, J.; Liu, X.; Wang, N. A brief review of alternative propellants and requirements for pulsed plasma thrusters in micropropulsion applications. *Chin. J. Aeronaut.* **2020**, *1000-9361*, 1–12. [CrossRef]
102. Polzin, K.; Martin, A.; Little, J.; Promislow, C.; Jorns, B.; Woods, J. State-of-the-Art and Advancement Paths for Inductive Pulsed Plasma Thrusters. *Aerospace* **2020**, *7*, 2–19. [CrossRef]
103. Lau, M.; Herdrich, G.; Grabe, M. Experimental Characterization of a Scalable Pulsed Magnetoplasmadynamic Propulsion System. In Proceedings of the European Space Propulsion Conference, Cologne, Germany, 19–22 May 2014.
104. Montag, C.; Herdrich, G.; Schönherr, T. Modifications and Experimental Analysis towards an Update of the Pulsed Plasma Thruster PETRUS. In Proceedings of the 35th International Electric Propulsion Conference, Atlanta, GA, USA, 8–12 October 2017.
105. Montag, C.; Herdrich, G.; del Amo, J.G.; Bauer, P.; Feyhl, D. PETRUS 2.0 PPT and its CubeSat-size PPU: Testing and Characterization. In Proceedings of the 36th International Electric Propulsion Conference, Vienna, Austria, 15–20 September 2019.
106. Wang, B.; Yang, W.; Tang, H.; Li, Z.; Kitaeva, A.; Chen, Z.; Cao, J.; Herdrich, G.; Zhang, K. Target thrust measurement for applied-field magnetoplasmadynamic thruster. *Meas. Sci. Technol.* **2018**, *29*, 1–10. [CrossRef]
107. Choueiri, E.Y. New Dawn for Electric Propulsion. *Sci. Am.* **2009**, *300*, 58–65. [CrossRef] [PubMed]
108. Coogan, W.J.; Choueiri, E. A Critical Review of Thrust Models for Applied-Field Magnetoplasmadynamic Thrusters. In Proceedings of the 53rd AIAA/SAE/ASEE Joint Propulsion Conference, Atlanta, GA, USA, 10–12 July 2017; pp. 1–27.
109. Coletti, M. A thrust formula for an MPD thruster with applied-magnetic field. *Acta Astronaut.* **2012**, *81*, 667–674. [CrossRef]
110. Wartelski, M.; Xavier, S. Method for Controlling the Temperature of an Electric Propulsion System. U.S. Patent Application No. WO/2018/007540, 1 November 2018.
111. Verma, A.; Ganguli, A.; Sahu, D.; Narayanan, R.; Tarey, R.D. Thrust evaluation of Compact ECR Plasma Source using 2-Zone global model and plasma measurements. *Plasma Sources Sci. Technol.* **2020**, *29*, 8–16. [CrossRef]
112. Ou, Y.; Wu, J.; Zhang, Y. Design and experimental results of a laser-ignited solid-propellant-fed magnetoplasmadynamic thruster. *Rev. Sci. Instruments* **2020**, *91*, 1. [CrossRef]
113. Wu, P.; Wang, Y.; Li, Y.; Wang, B.; Zhang, K.; Tang, H.; Cao, J. Cathode erosion site distributions in an applied-field magnetoplasmadynamic thruster. *Plasma Sci. Technol.* **2020**, *22*, 7. [CrossRef]
114. Zolotukhin, D.; Daniels, K.; Keidar, M. Discharge characteristics of two-stage micro-cathode arc MPD thrusters with a permanent magnet and a pulsed magnetic field. *J. Appl. Phys.* **2020**, *54*, 1. [CrossRef]

115. List, M.; Bremer, S.; Rievers, B.; Selig, H. Modelling of Solar Radiation Pressure Effects: Parameter Analysis for the MICROSCOPE Mission. *Int. J. Aerosp. Eng.* **2015**, *2015*, 3–11. [CrossRef]
116. Spencer, D.A.; Betts, B.; Bellardo, J.M.; Diaz, A.; Plante, B.; R.Mansell, J. The LightSail 2 solar sailing technology demonstration. *Adv. Space Res.* **2020**, , 1–8. [CrossRef]
117. Atwater, H.A.; Davoyan, A.R.; Ilic, O.; Jariwala, D.; Sherrott, M.C.; Went, C.M.; Whitney, W.S.; Wong, J. Materials challenges for the Starshot lightsail. *Nat. Mater.* **2018**, *17*, 861–867. [CrossRef] [PubMed]
118. Yuan, S.; Fan, W.; Jin, Y.; Wang, D.; Liu, T. Free-standing flexible graphene-based aerogel film with high energy density as an electrode for supercapacitors. *Nano Mater. Sci.* **2020**, 1–15. [CrossRef]
119. Heller, R.; Anglada-Escudé, G.; Hippke, M.; Kervella, P. Low-cost precursor of an interstellar mission. *Astron. Astrophys.* **2020**, *641*, 1. [CrossRef]
120. Parker, J.; Peterson, C.W.; Yifat, Y.; Rice, S.A.; Yan, Z.; Gray, S.K.; Scherer, N.F. Optical matter machines: Angular momentum conversion by collective modes in optically bound nanoparticle arrays. *Optica* **2020**, *7*, 1341. [CrossRef]
121. Phipps, C.; Birkan, M.; Bohn, W.; Horisawa, H.A.E.A.H.; Lippert, T.; Michaelis, M.; Rezunkov, Y.; Sasoh, A.; Schall, W.; Scharring, S.; et al. Review: Laser-Ablation Propulsion. *J. Propuls. Power* **2010**, *26*, 611–632. [CrossRef]
122. Voss, S.S. Nuclear Security Considerations for Space Nuclear Power: A Review of Past Programs with Recommendations for Future Criteria. *Nucl. Technol.* **2019**, *206*, 1097–1108. [CrossRef]
123. Ching-ShengLin.; Youinou, G.J. *Design and Analysis of a 250 MW Plate-Fuel Reactor for Nuclear Thermal Propulsion*; U.S. Department of Energy Office of Scientific and Technical Information: Oak Ridge, TN, USA, 2020.
124. Tenneti, A.; Hampika, G.; Rohit, V.; Guduri, M. Interstellar Space Travel Using Nuclear Propulsion. *Energy Syst. Drives Autom.* **2019**, *664*, 331. [CrossRef]
125. Bahmani, J. Reduction in inertial confinement fusion ignition energy of3He-3He plasma by laser-accelerated deuterons. *Hydrog. Energy* **2020**, *45*, 16672–16676. [CrossRef]
126. Giuffrida, L.; Belloni, F.; Margarone, D.; Petringa, G.; Milluzzo, G.; Scuderi, V.; Velyhan, A.; Rosinski, M.; Picciotto, A.; et al. High-current stream of energetic α particles from laser-driven proton-boron fusion. *Phys. Rev. E.* **2020**, *101*, 1–10. [CrossRef] [PubMed]
127. Vyas, A.C.; Cassibry, J.T. Numerical modelling of compact toroid formation and propagation for magneto-inertial fusion research. In Proceedings of the AIAA Propulsion and Energy 2020 Forum, Virtual Event, 24–28 August 2020; . [CrossRef]
128. Litchford, R.J. *Prospects for Interstellar Propulsion*; Space Technology Mission Directorate, NASA: Washington, DC, USA, 2020.
129. White House. *A New Era for Deep Space Exploration and Development*; National Space Council: Huntsville, AL, USA, 26 March 2020
130. Raj, J.K.; Parks, G. Development of a deep space nuclear electric propulsion (NEP)system –a NuAER plasma NEP reactor. In Proceedings of the AIAA Propulsion and Energy 2020 Forum, Virtual Event, 24–28 August 2020; pp. 1–14. [CrossRef]
131. Torres, A.S. Radioisotope Power Systems for Space Applications. *Appl. Phys. Sci.* **2010**,*12*, 457–471. [CrossRef]
132. Howe, T.M.H.S.; Miller, J.R. Advanced Thermoelectric Power Generation System for Low Enriched Uranium Fuel Reactors. *Int. Conf. Environ. Syst.* **2020**, 1–11. Available online: https://ttu-ir.tdl.org/bitstream/handle/2346/86284/ICES-2020-180.pdf?sequence=1 (accessed on 3 November 2020).
133. Lappas, V.; Tsourdos, A.; Kindylides, S.; Kostopoulos, V. A Low Cost Thermoelectric Generator for Small Satellites. In Proceedings of the AIAA Scitech 2019 Forum, San Diego, CA, USA, 7–11 January 2019. [CrossRef]
134. He, S.; Xia, Y.; Xu, F.; Zhou, L.; Quyang, X. A Nuclear Decay Micropropulsion Technology Based on Spontaneous Alpha Decay. *Nucl. Sci. Eng.* **2020**, 1–6. [CrossRef]
135. Musinski, L.; Liu, T.; Gilchrist, B.; Gallimore, A.; Keidar, M. Experimental Results and Modeling Advances in the Study of the Nanoparticle Field Extraction Thruster. In Proceedings of the 43rd AIAA/ASME/SAE/ASEE Joint Propulsion Conference & Exhibit, Cincinnati, OH, USA, 8–11 July 2007. [CrossRef]
136. Sullivan, D.; Kline, J.; Philippe, C.; Micci, M. Current status of the microwave arcjet thruster. In Proceedings of the 31st Joint Propulsion Conference and Exhibit, San Diego, CA, USA, 10–12 July 1995; pp. 1–8. [CrossRef]
137. Yildiz, M.S. Experimental Performance Analysis of the BUSTLab Microwave Electrothermal Thruster. In Proceedings of the 52nd AIAA/SAE/ASEE Joint Propulsion Conference, Salt Lake City, UT, USA, 25–27 July 2016. [CrossRef]
138. Squire, J.P.; Carter, M.; Diaz, F.R.C.; Corrigan, A.; Dean, L.; Farrias, J.; Giambusso, M.; McCaskill, G.; Yao, T. Steady-state Testing at 100 kW in the VASIMR®VX-200SS Project. In Proceedings of the AIAA Propulsion and Energy 2019 Forum, Indianapolis, IN, USA, 19–22 August 2019; pp. 1–10. [CrossRef]
139. Bathgate, S.; BILEKD, M.M.M.; MCKENZIE, R. Electrodeless plasma thrusters forspacecraft: A review. *Plasma Sci. Technol.* **2017**, *19*, 24. [CrossRef]
140. Frisbee, R.H.; Mikellides, I.G. The Nuclear-Electric Pulsed Inductive Thruster (NuPIT):Mission Analysis for Prometheus. In Proceedings of the 41st AIAA/ASME/SAE/ASEE Joint Propulsion Conference, Tucson, AZ, USA, 10–13 July 2005.
141. West, J.L.M.D.; Lafleur, T.; Charles, C.; Boswell, R.W. Thrust measurements in a low-magnetic field high-density mode in the helicon double layer thruster. *J. Phys. D Appl. Phys.* **2010**, *43*, 2–8. [CrossRef]
142. Romano, F.; Chan, Y.A.; Herdrich, G.; Traub, C.; Fasoulas, S.; Roberts, P.C.E.; Smith, K.; Edmondson, S.; Haigh, S.; Crisp, N.H.; et al. RF Helicon-based Inductive Plasma Thruster (IPT) Design for an Atmosphere-Breathing Electric Propulsion system (ABEP). *Acta Astronaut.* **2020**, *176*, 476–483. [CrossRef]

143. Churaman, W.; Morris, C.J.; Currano, L.J.; Bergbreiter, S. On-chip porous silicon microthruster for robotic platforms. In Proceedings of the 17th International Conference on Solid-State Sensors, Actuators and Microsystems, Barcelona, Spain, 16–20 June 2013; pp. 1599–1602. [CrossRef]
144. Manchester, Z.R.; Peck, M. Stochastic Space Exploration with Microscale Spacecraft. In Proceedings of the AIAA Guidance, Navigation, and Control Conference, Portland, Oregon, 8–11 August 2011. [CrossRef]
145. Hu, W.; Welch, C.; Ancona, E. A Minimal Chipsat Interstellar Mission: Technology and Mission Architecture. In Proceedings of the 69th International Astronautical Congress, Bremen, Germany, 1–5 October 2018.
146. Liu, J.; Li, G.; Zhu Zheng, H.; Zhan, X. Orbital boost characteristics of spacecraft by electrodynamic tethers with consideration of electric-magnetic-dynamic energy coupling. *Acta Astronaut.* **2020**, *171*, 196–207. [CrossRef]
147. Liu, J.; Li, G.; Zhu Zheng, H.; Liu, M.; Zhan, X. Automatic orbital maneuver for mega-constellations maintenance with electrodynamic tethers. *Aerosp. Sci. Technol.* **2020**, *105*, 1–8. [CrossRef]
148. Pietzka, M. Development and Characterization of a Propulsion System for CubeSats Based on Vacuum Arc Thrusters. Ph.D. Thesis, Munich University, Munich, Germany, 2016; pp. 2–16. Available online: http://d-nb.info/1115728423 (accessed on 3 November 2020).
149. Li, Y.H.; Pan, J.Y.; Herdrich, G. Design and demonstration of micro-scale vacuum cathode arc thruster with inductive energy storage circuit. *Acta Astronaut.* **2020**, *172*, 33–46. [CrossRef]
150. Kolbeck, J.; Anders, A.; Beilis, I.I.; Keidar, M. Micro-propulsion based on vacuum arcs. *J. Appl. Phys.* **2019**, *125*, 1–10. [CrossRef]
151. Chan, Y.A.; Herdrich, G. Influence of Cathode Dimension on Discharge Characteristics of Inertial Electrostatic Confinement Thruster. In Proceedings of the 36th International Electric Propulsion Conference, Vienna, Austria, 15–20 September 2019; pp. 1–8.
152. Chan, Y.A.; Herdrich, G. Inertial Electrostatic Confinement: Innovation for Electric Propulsion and Plasma Systems. In Proceedings of the 35th International Electric Propulsion Conference, Atlanta, GA, USA, 8–12 October 2017; pp. 1–9.
153. Bok, C.B.; Comeau, A.; Dolgopolov, A.; Halt, T.; Juang, C.; Smith, P. *SmallSats by the Numbers*; Bryce and Space Technology. 2020; pp. 5–10. Available online: https://brycetech.com/reports/report-documents/Bryce_Smallsats_2020.pdf (accessed on 4 November 2020).